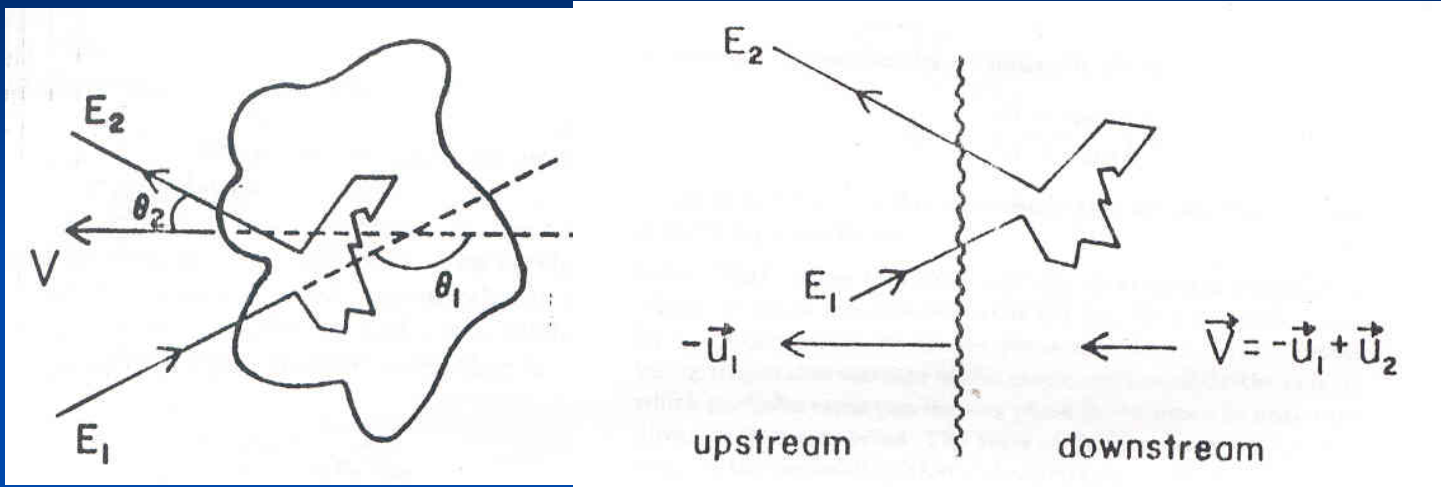


Lecture 17 101218

Il pdf delle lezioni puo' essere scaricato da
[http://www.fisgeo.unipg.it/~fiandrin/didattica_fisica/
cosmic_rays1819/](http://www.fisgeo.unipg.it/~fiandrin/didattica_fisica/cosmic_rays1819/)

SW energy gain: another approach

Let consider another approach: the same physical mechanism is working both at a shock front both in a cloud of magnetized plasma with strong magnetic irregularities acting as collisionless scattering centers (e.g. this can be thought as the turbulent region ahead a shock front or even the whole galactic disk)



Downstream the shocked gas flows to the left with speed u_2 relative to the shock front \rightarrow in the lab it moves to the left with $V = -u_1 + u_2$

In the rest frame of the moving cloud or in the shock rest frame, we have

$$E'_1/c = \gamma(E_1/c - \beta_V p_{x1}) = \gamma(E_1/c)(1 - \beta_V \cos \theta_1) \quad \text{Because for ultra-relat. particles } E/c=p$$

The collisions are elastic (because collision-less in the rest frame of the cloud/SW)

$E'_1 = E'_2$ and going back to the labo

$$E_2/c = \gamma(E'_2/c + \beta_V p'_{x2}) = \gamma(E'_2/c)(1 + \beta_V \cos \theta'_2) = \gamma(E'_1/c)(1 + \beta_V \cos \theta'_2)$$

$$= \gamma^2(E_1/c)(1 - \beta_V \cos \theta_1)(1 + \beta_V \cos \theta'_2) = \gamma^2[(E_1/c)(1 + \beta_V \cos \theta'_2 - \beta_V \cos \theta_1 - \beta_V^2 \cos \theta_1 \cos \theta'_2)]$$

therefore
$$\frac{\Delta E}{E} = \frac{E_2 - E_1}{E_1} = \gamma^2(1 + \beta_V \cos \theta'_2 - \beta_V \cos \theta_1 - \beta_V^2 \cos \theta_1 \cos \theta'_2) - 1$$

SW energy gain: another approach

$$\frac{\Delta E}{E} = \frac{E_2 - E_1}{E_1} = \gamma^2(1 + \beta_V \cos \theta'_2 - \beta_V \cos \theta_1 - \beta_V^2 \cos \theta_1 \cos \theta'_2) - 1$$

The crucial difference between the two cases comes when we take the angular averages to obtain the average fractional energy gain per encounter.

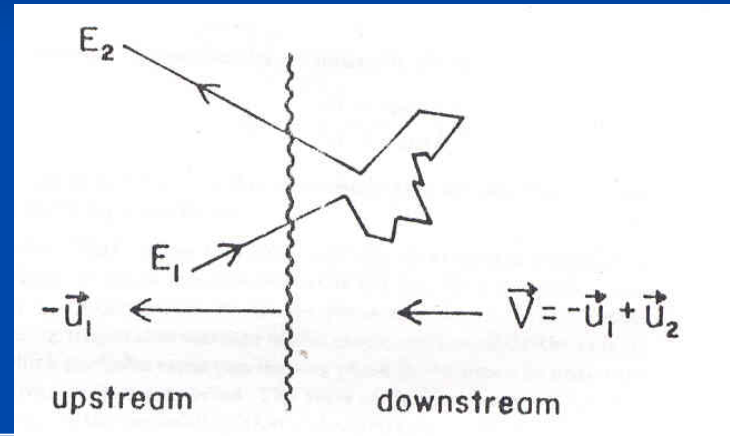
First, the average over θ'_2 has to be done

Cloud

In S' (where the particle is at rest in average), the particle distr. is isotropic because of the random motion inside the cloud, therefore $dn/d(\cos \theta'_2) = \text{const.}$, $-1 < \cos \theta'_2 < 1$

Then $\langle \cos \theta'_2 \rangle = 0$ and

$$\Delta E/E_1 = \gamma^2 (1 - \beta_V \cos \theta_1) - 1$$

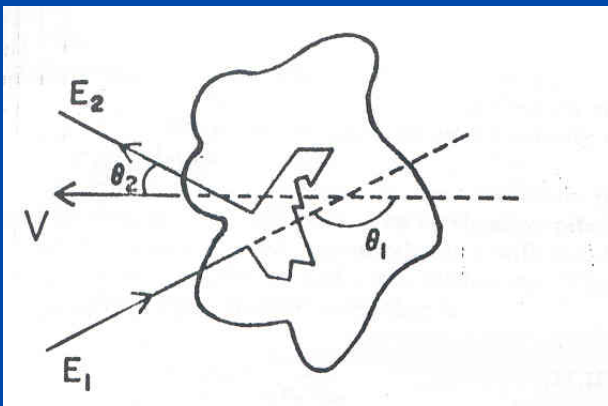


Shock front

In S' we have again a isotropic distr. but we have to project on a plane (the shock front), therefore $dn/d(\cos \theta'_2) = 2 \cos \theta'_2$, $0 < \cos \theta'_2 < 1$

Then $\langle \cos \theta'_2 \rangle = 2/3$ and

$$\Delta E/E_1 = \gamma^2 [1 + (2/3)\beta_V - \beta_V \cos \theta_1 - (2/3)\beta_V^2 \cos \theta_1] - 1$$



SW energy gain: another approach

Shock front

In S' we have again a isotropic distr. but we have to project on a plane (the shock front), therefore

$$dn/d(\cos\theta_2') = 2\cos\theta_2', \quad 0 < \cos\theta_2' < 1$$

Then $\langle \cos\theta_2' \rangle = 2/3$ and

$$\Delta E/E_1 = \gamma^2 [1 + (2/3)\beta_V - \beta_V \cos\theta_1 - (2/3)\beta_V^2 \cos\theta_1] - 1$$

The prob of the particles which cross the shock arrive in a solid angle $d\Omega$ around θ dir per unit of time is:

$$dn \propto v \cos\theta d\Omega dt \rightarrow dp(\theta) \propto \cos\theta d(\cos\theta)$$

Normalizing so that prob is 1 for all the particles approaching the shock (ie those with $0 < \theta < \pi/2$) one gets

$$dp(\theta) = 2\cos\theta d(\cos\theta)$$

SW energy gain: another approach

Next we need to average over $\cos\theta_1$

Cloud

The probability of a collision is \sim to the relative speed between the cloud and the particle

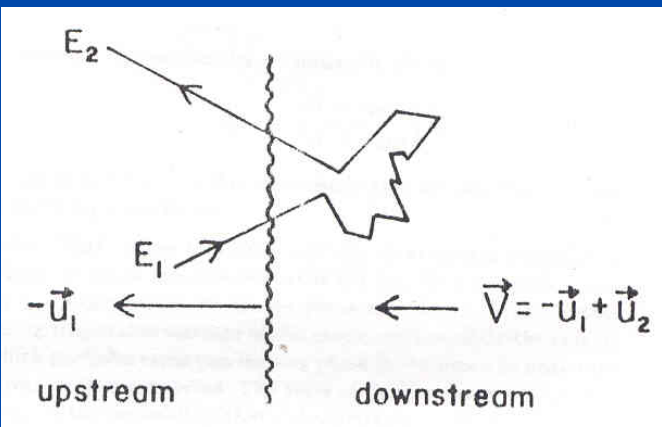
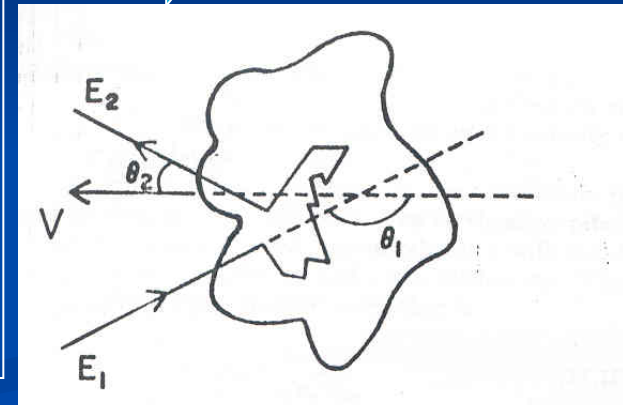
$$dn/d(\cos\theta_1) = (c - V\cos\theta_1)/2c, \quad -1 < \cos\theta_1 < 1$$

Then $\langle \cos\theta_1 \rangle = -\beta_V/3$ and

$$\begin{aligned} \Delta E/E_1 &= \gamma^2 (1 - \beta_V \cos\theta_1) - 1 = (1 + \beta_V^2/3)/(1 - \beta_V^2) - 1 = \\ &= (4/3)\gamma^2 \beta_V^2 \approx (4/3)\beta_V^2 \text{ if } \beta_V \ll 1 \end{aligned}$$



2nd order



1st order



Shock front

We have again a isotropic distr. but we have to project on a plane (the shock front), therefore

$$dn/d(\cos\theta_1) = 2 \cos\theta_1, \quad -1 < \cos\theta_1 < 0$$

Then $\langle \cos\theta_1 \rangle = -2/3$ and

$$\begin{aligned} \Delta E/E_1 &= \gamma^2 [1 + (4/3)V - (4/9)V^2] - 1 = \\ &= \gamma^2 [(4/3)\beta + (5/9)\beta^2] \sim (4/3)\beta \text{ if } \beta \ll 1 \end{aligned}$$

$$v_{\text{rel}} = |\vec{v}_{\text{cloud}} - \vec{v}_{\text{particle}}|$$

$$= \sqrt{(c - v \cos \theta_i)^2 + v^2 \sin^2 \theta_i}$$

$$= c \sqrt{(1 - \beta \cos \theta_i)^2 + \beta^2 \sin^2 \theta_i}$$

$$= c \sqrt{1 + \beta^2 - 2\beta \cos \theta_i}$$

$$\simeq c \sqrt{1 - 2\beta \cos \theta_i}$$

$$\simeq c (1 - \beta \cos \theta_i)$$

$$\beta \ll 1$$

Spectrum of accelerated particles

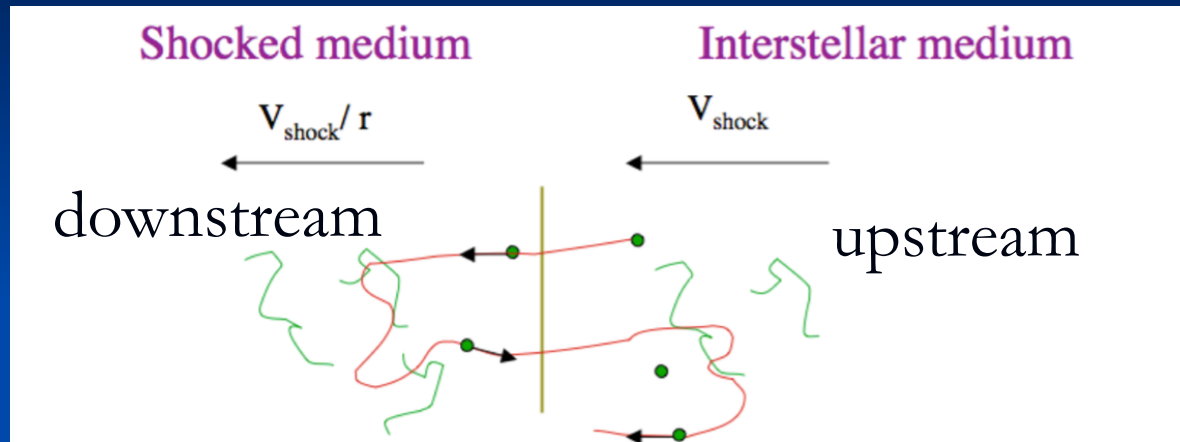
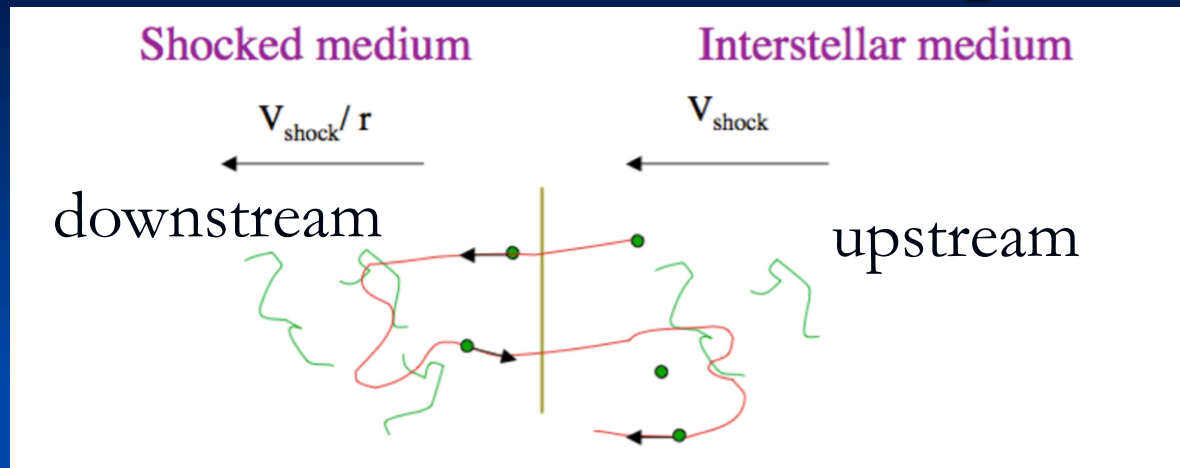


FIG. 3.9: Schematic view of a cycle as seen in the shock rest frame : the particle initially in the ISM (upstream medium) enters the shocked medium (downstream medium), it is then isotropized by the magnetic turbulence and reflected back to the upstream medium where the particle is isotropized again and eventually crossed the shock to start a new cycle.

After calculating the mean energy gain obtained after a single cycle upstream \rightarrow downstream \rightarrow upstream, one can try to estimate the number of cycles this particles are going to achieve before "leaving the system". At first place, it is important to understand what mechanism is going to limit the number of cycles a particle can perform. The critical point is that during each cycle a given has a probability not to come back to the shock, in other word a probability to escape from "the acceleration region".

Spectrum of accelerated particles



Within our hypothesis (infinite media upstream and downstream and steady state), the particles have no way of escaping upstream of the shock. Indeed since by hypothesis the accelerated particles are isotropized by the ambient magnetic fields the accelerated particles fluid has no net velocity with respect to the medium (either downstream or upstream) rest frame. As in the upstream medium frame the shock is "going after the particles", the return probability at the shock is 1, meaning that the escape probability is 0. In the downstream medium on the other hand, the cosmic-ray fluid has a zero velocity with respect to the ambient medium and the shock is going away with a velocity $v_2 = v_{sh}/r$. This means that the accelerated particles fluid is in average slowly advected away from the shock. The escape probability can be estimated by comparing the flux of particles being advected far away from the shock with the flux of particle entering the downstream medium by crossing the shock from the upstream medium. Before performing this trivial calculation, we can give an alternative reasoning to understand the impossibility of leaving the system in the upstream frame.

Spectrum of accelerated particles

Let us now consider individual particles rather than the "accelerated particles fluid" and let's think in term of diffusion as we did in the chapter dedicated to Galactic cosmic-rays. Let us assume a particle enters the upstream medium (crossing the shock from upstream) at $t = 0$. Since we have an infinite amount of time available and since the upstream medium is infinite (at least in the framework of our hypotheses) diffusion theory tells us that the probability for the particle to come back to the plane where it crossed the shock within the infinite amount of time available is 1. Then the probability to cross the shock again would be 1 even if the shock was not moving. The fact that the shock is going after the particle in the upstream medium makes it even easier for the particle to cross the shock again.

Downstream, the probability for the particle to come back to the plane where it crossed the shock (from upstream) is still one, but the problem is that during the time it took for the particle to come back, the shock has moved away. If one calculated, using diffusion theory, the probability for a particle, not only to come back to where it last crossed the shock, but where the shock actually is at a given time t between 0 and ∞ (which is actually the condition for the particle to come back to the shock and be able to cross it again and which is, unlike in the upstream medium, a more stringent condition than just coming where it last crossed the shock) then one would find a probability smaller than 1, as a result of the shock going away with respect to the downstream fluid frame.

Spectrum of accelerated particles

Let us now calculate the escape probability using our first reasoning in terms of accelerated particles fluid. Let n_0 be the accelerated particle density. Due to the global advection of the downstream fluid away from the shock front with a velocity v_2 , the flux of accelerated particles passing through a unit surface very far away from the shock is $\phi_{esc} = n_0 v_2$. On the other hand the flux of particles crossing the shock from upstream to downstream is given by :

$$\phi_{ud} = \frac{n_0}{2} v_{part} \int_{\pi/2}^{\pi} \cos \theta \sin \theta d\theta = \frac{n_0}{4} v_{part} \simeq \frac{n_0}{4} c \quad (3.36)$$

The escape probability is then simply the ratio of the two fluxes :

$r = \rho_2/\rho_1 = u_1/u_2$ is the shock compression ratio

$$P_{esc} = \frac{\phi_{esc}}{\phi_{ud}} \simeq \frac{4}{r} \beta_{sh} \quad (3.37)$$

We then have obtained so far $\langle \Delta E \rangle = \frac{4}{3} \left(\frac{r-1}{r} \right) \beta_{sh} E = kE$ and $P_{esc} = \frac{4}{r} \beta_{sh}$. We have everything we need to predict the slope of the accelerated particle spectrum :

Spectrum of accelerated particles

After 1 cycle, the mean energy of particles injected with the energy E_0 is :

$$E_1 = (1 + k)E_0 \quad (3.38)$$

thus after n cycles :

$$E_n = (1 + k)^n E_0 \Leftrightarrow n = \frac{\ln(E/E_0)}{\ln(1 + k)} \quad (3.39)$$

on the other hand, if we initially injected N_0 particles then after n cycles we have :

$$N_n = N_0(1 - P_{esc})^n = N_0(1 - P_{esc})^{\frac{\ln(E/E_0)}{\ln(1+k)}} = N(\geq E_n) \quad (3.40)$$

the right hand side just meaning that particles which have achieved n end up with energies greater or equal to E_n (since they will either escape at the cycle or continue for more cycles). Using $a^{\ln b} = e^{\ln a \ln b} = b^{\ln a}$ and dropping the subscript n we get :

$$N(\geq E) = N_0 \left(\frac{E}{E_0} \right)^{\frac{\ln(1-P_{esc})}{\ln(1+k)}} \quad (3.41)$$

Spectrum of accelerated particles

and since the shock is non-relativistic, $\beta_{sh} \ll 1 \Leftrightarrow P_{esc} \ll 1$ and $k \ll 1$:

Taylor's expansion of exponent

$$\begin{aligned} \ln(1 - P_{esc}) &\approx -P_{esc} \\ \ln(1 + k) &\approx k \end{aligned} \quad N(\geq E) = N_0 \left(\frac{E}{E_0} \right)^{\frac{-P_{esc}}{k}} \quad (3.42)$$

moreover

$$N(\geq E) = \int_E^{+\infty} n(E) dE \quad (3.43)$$

where $n(E)dE$ is the number of particles with energy between E and $E + dE$ and is the quantity we are looking for. Then,

$$r = \rho_2 / \rho_1 = u_1 / u_2 \quad n(E) = \left| \frac{dN(\geq E)}{dE} \right| = (x - 1) \frac{N_0}{E_0} \left(\frac{E}{E_0} \right)^{-x} \quad (3.44)$$

with (after developing P_{esc}/k),

$$x = \frac{r + 2}{r - 1} \quad (3.45)$$

We obtain a power law spectrum with a *spectral index* x depending only on the shock compression ratio r ! For a monoatomic gas and a strong shock ($\gamma_a = 5/3$, $M_1 \gg 1$), the slope of the power law is $x = 2$ and is "universal"⁵.

The Diffusion-Convection Equation: A more formal approach

ADIABATIC COMPRESSION
OR SHOCK COMPRESSION



$$\frac{\partial f}{\partial t} = \frac{\partial}{\partial x} \left[D \frac{\partial f}{\partial x} \right] - u \frac{\partial f}{\partial x} + \frac{1}{3} \frac{du}{dx} p \frac{\partial f}{\partial p} + Q(x, p, t)$$

INJECTION
TERM

ADVECTION
WITH THE
FLUID

SPATIAL DIFFUSION

■ $f(r, p, t)$ is the particle distribution function

■ Number density is $n(r, p, t) dp = 4\pi p^2 f$

$$f_0(p) = \frac{3u_1}{u_1 - u_2} \frac{N_{inj}}{4\pi p_{inj}^2} \left(\frac{p}{p_{inj}} \right)^{\frac{-3u_1}{u_1 - u_2}}$$

The solution is a power law in momentum

The slope depends ONLY on the compression ratio (not on the diffusion coef.)

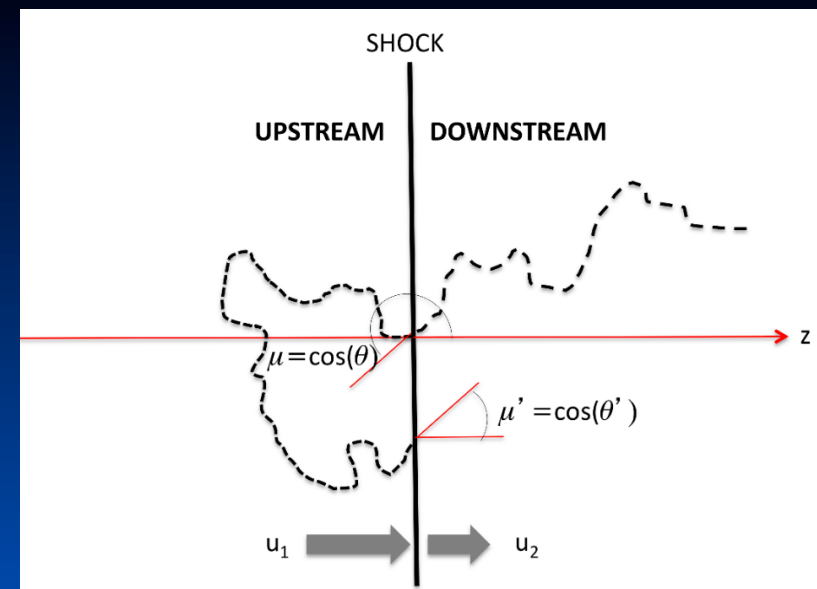
Injection momentum and efficiency are free param

The diffusion approach

There remains the second type of motion, that of the individual centres relative to the background. If this has a systematic component it should obviously be added to the background velocity U (the energetic particles cannot see the background directly, they can only sense the mean velocity of the scattering centres). The residual random component causes each particle to have its momentum changed by a random amount of the order of $\Delta \mathbf{p} \sim p \, V / v$ at each scattering where V is the velocity of a centre. This gives a term that describes the momentum (or energy) gain/loss of the distribution

$$\frac{\partial f}{\partial t} = \frac{\partial}{\partial x} \left[D \frac{\partial f}{\partial x} \right] - u \frac{\partial f}{\partial x} + \boxed{\frac{1}{3} \frac{du}{dx} p \frac{\partial f}{\partial p}} + Q(x, p, t)$$

The diffusion approach



For a stationary parallel shock, namely a shock for which the normal to the shock is parallel to the orientation of the background magnetic field (see Fig. 6) the transport of particles is described by the diffusion-convection equation (Skilling, 1975a) (see (Blandford and Eichler, 1987) for a detailed derivation), which in the shock frame reads: Stationary shock means steady state solutions, $\partial f / \partial t = 0$

$$u \frac{\partial f}{\partial z} = \frac{\partial}{\partial z} \left[D \frac{\partial f}{\partial z} \right] + \frac{1}{3} \frac{du}{dz} p \frac{\partial f}{\partial p} + Q, \quad (34)$$

where $f(z, p)$ is the distribution function of accelerated particles, normalized in a way that the number of particles with momentum p at location z is $\int dp 4\pi p^2 f(p, z)$. In Eq. 34 the LHS is the convection term, the first term of the RHS is the spatial diffusion term. The second term on the RHS describes the effect of fluid compression on the accelerated particles, while $Q(x, p)$ is the injection term.

THE TRANSPORT EQUATION APPROACH

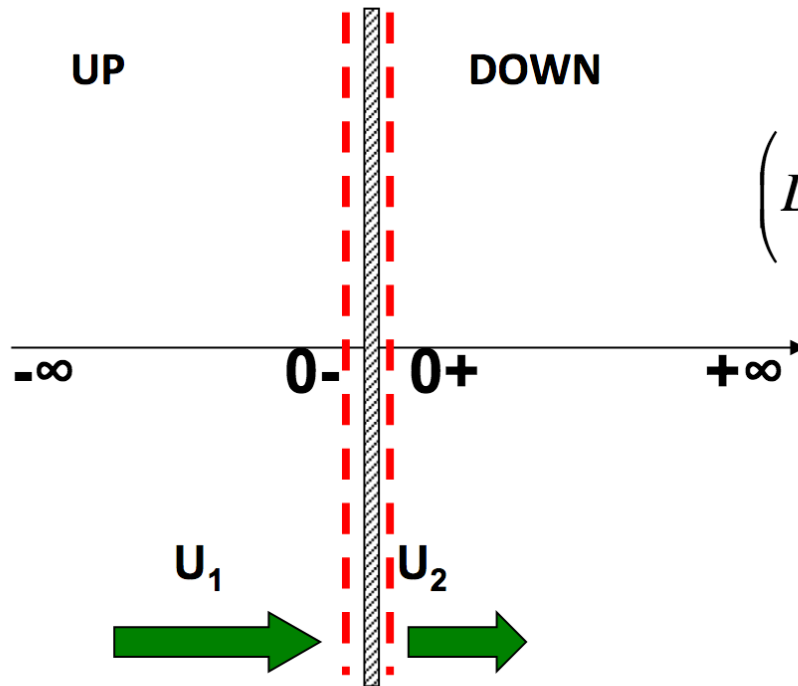
$$\frac{\partial f}{\partial t} = \frac{\partial}{\partial x} \left[D \frac{\partial f}{\partial x} \right] - u \frac{\partial f}{\partial x} + \frac{1}{3} \frac{du}{dx} p \frac{\partial f}{\partial p} + Q(x, p, t)$$

DIFFUSION

ADVECTION

COMPRESSION

INJECTION



Integrating around the shock:

$$\left(D \frac{\partial f}{\partial x} \right)_2 - \left(D \frac{\partial f}{\partial x} \right)_1 + \frac{1}{3} (u_2 - u_1) p \frac{df_0(p)}{dp} + Q_0(p) = 0$$

Integrating from upstr. infinity to 0^- :

$$\left(D \frac{\partial f}{\partial x} \right)_1 = u_1 f_0$$

and requiring homogeneity downstream:

$$p \frac{df_0}{dp} = \frac{3}{u_2 - u_1} (u_1 f_0 - Q_0)$$

A few comments on Eq. 34 are in order: 1) the shock will appear in this equation only in terms of a boundary condition at $z = 0$, and the shock is assumed to have infinitely small size along z . This implies that this equation cannot properly describe the thermal particles in the fluid. The distribution function of accelerated particles is continuous across the shock. 2) In a self-consistent treatment in which the acceleration process is an integral part of the processes that lead to the formation of the shock one would not need to specify an injection term. Injection would result from the microphysics of the particle motions at the shock. This ambiguity is usually faced in a phenomenological way, by adopting recipes such as the thermal leakage one (Malkov, 1998; Gieseler et al, 2000) that allow one to relate the injection to some property of the plasma behind the shock. This aspect becomes relevant only in the case of non-linear theories of DSA, while for the test particle theory the injection term only determines the arbitrary normalization of the spectrum. However it is worth recalling that while these recipes may apply to

the case of protons as injected particles, the injection of heavier nuclei may be much more complex. In fact, it has been argued that nuclei are injected at the shock following the process of sputtering of dust grains (Meyer et al, 1997; Ellison et al, 1997).

For the purpose of the present discussion I will assume that injection only takes place at the shock surface, immediately downstream of the shock, and that it only consists of particles with given momentum p_{inj} :

$$Q(p, x) = \frac{\eta n_1 u_1}{4\pi p_{inj}^2} \delta(p - p_{inj}) \delta(z) = q_0 \delta(z), \quad (35)$$

where n_1 and u_1 are the fluid density and fluid velocity upstream of the shock and η is the acceleration efficiency, defined here as the fraction of the incoming number flux across the shock surface that takes part in the acceleration process. Hereafter I will use the indexes 1 and 2 to refer to quantities upstream and downstream respectively.

The key here is that a parallel shock does nothing locally to energetic particles; there is no discontinuity in the magnetic field and the particles simply continue their helical paths across the front. Thus the complete momentum space distribution function, as measured in the shock frame, must be continuous across the front.

The spatial distribution of the source term is arbitrary (or determined by the observations, if feasible)

The diffusion approach

The compression term vanishes everywhere but at the shock since $du/dz = (u_2 - u_1)\delta(z)$. Integration of Eq. 34 around the shock surface (between $z = 0^-$ and $z = 0^+$) leads to:**

$$\left[D \frac{\partial f}{\partial z} \right]_2 - \left[D \frac{\partial f}{\partial z} \right]_1 + \frac{1}{3}(u_2 - u_1)p \frac{df_0}{dp} + q_0(p) = 0, \quad (36)$$

where $f_0(p)$ is now the distribution function of accelerated particles at the shock surface. Particle scattering downstream leads to a homogeneous distribution of particles, at least for the case of a parallel shock, so that $[\partial f / \partial z]_2 = 0$. In the upstream region, where $du/dz = 0$ the transport equation reduces to:

$$\frac{\partial}{\partial z} \left[u f - D \frac{\partial f}{\partial z} \right] = 0, \quad \text{Quantity in parenthesis is constant. Since must go to 0 when } z \rightarrow -\infty, \text{ it must be zero everywhere}$$

and since the quantity in parenthesis vanishes at upstream infinity, it follows that

$$\left[D \frac{\partial f}{\partial z} \right]_1 = u_1 f_0. \quad (38)$$

At the shock front upstream, $[D(\partial f / \partial z)]_1 - [u f]_1 = 0$. But $u = u_1$ and $f \rightarrow f_0$ at 0^- and therefore (38) holds

** Integration at the eshock

$$\int_{-\varepsilon}^{+\varepsilon} dz \left[\frac{\partial}{\partial z} \left[D \frac{\partial f}{\partial z} \right] - u \frac{\partial f}{\partial z} + \frac{1}{3} \frac{du}{dz} p \frac{\partial f}{\partial p} + Q(z, p, t) \right]$$

f is continuous at shock (in $[-\varepsilon, +\varepsilon]$)

$$du/dz = (u_2 - u_1) \delta(z)$$

$$Q(z, p, t) = q_0(p) \delta(z)$$

$$\int_{-\varepsilon}^{+\varepsilon} dz \left[\frac{\partial}{\partial z} \left[D \frac{\partial f}{\partial z} \right] - u \frac{\partial f}{\partial z} + \frac{1}{3} (u_2 - u_1) \delta(z) p \frac{\partial f}{\partial p} + q_0(p) \delta(z) \right]$$

The contribution from $\partial f / \partial z$ is $= 0$, as can be seen integrating by parts due to the continuity of f

$$\left[D \frac{\partial f}{\partial z} \right]_2 - \left[D \frac{\partial f}{\partial z} \right]_1 + \frac{1}{3} (u_2 - u_1) p \frac{\partial f_0}{\partial p} + q_0(p)$$

f_0 is the distribution at the shock (due to the $\delta(z)$) and represents the distribution function of the accelerated particles

The diffusion approach

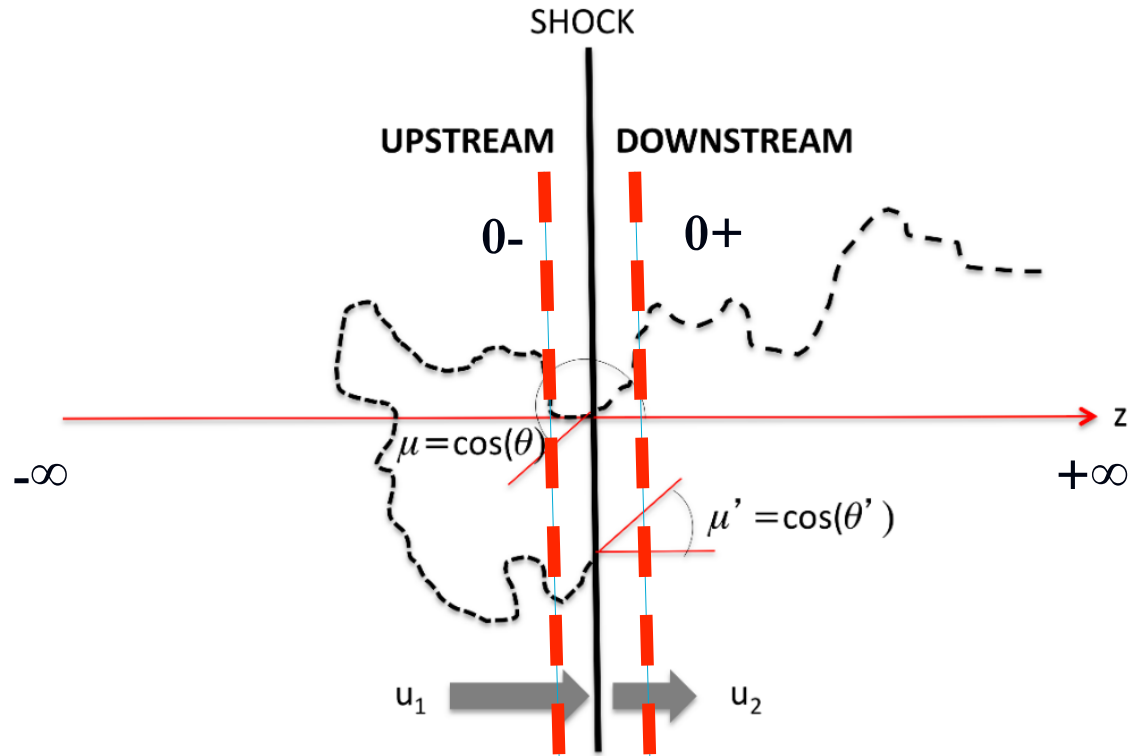


Fig. 6 Illustration of test-particle acceleration at a collisionless shock. In the shock frame the plasma enters from the left with velocity u_1 and exits to the right with velocity $u_2 < u_1$. Here the test particle is shown to enter downstream with cosine of the pitch angle μ (as measured in the upstream plasma frame) and exit with a cosine of the pitch angle μ' (as measured in the downstream plasma frame).

The diffusion approach

Using this result in Eq. 36 we obtain an equation for $f_0(p)$

$$u_1 f_0 = \frac{1}{3}(u_2 - u_1)p \frac{df_0}{dp} + \frac{\eta n_1 u_1}{4\pi p_{inj}^2} \delta(p - p_{inj}), \quad *** \quad (39)$$

which is easily solved to give: The shock compression ratio $r = \rho_2/\rho_1 = u_1/u_2$

$$f_0(p) = \frac{3r}{r-1} \frac{\eta n_1}{4\pi p_{inj}^2} \left(\frac{p}{p_{inj}} \right)^{-\frac{3r}{r-1}}. \quad (40)$$

The spectrum of accelerated particles is a power law in momentum (and not in energy as is often assumed in the literature) with a slope α that only depends on the compression ratio r :

$$\alpha = \frac{3r}{r-1}. \quad (41)$$

The slope tends asymptotically to $\alpha = 4$ in the limit $M_s \rightarrow \infty$ of an infinitely strong shock front. The number of particles with energy ϵ is $n(\epsilon)d\epsilon = 4\pi p^2 f_0(p)(dp/d\epsilon)d\epsilon$, therefore $n(\epsilon) \propto \epsilon^{-\alpha}$ for relativistic particles and $n(\epsilon) \propto \epsilon^{(1-\alpha)/2}$ for non-relativistic particles. In the limit of strong shocks, $n(\epsilon) \propto \epsilon^{-2}$ ($n(\epsilon) \propto \epsilon^{-3/2}$) in the relativistic (non-relativistic) regime.

*** solution

$$u_1 f_0 = \frac{1}{3}(u_2 - u_1)p \frac{df_0}{dp} + \frac{\eta n_1 u_1}{4\pi p_{inj}^2} \delta(p - p_{inj})$$

Dividing by u_1 both sides and using the definition of r

$$f_o = \frac{1}{3}\left(\frac{1}{r} - 1\right)p \frac{df_o}{dp} + \frac{\eta n_1}{4\pi p_{inj}^2} \delta(p - p_{inj})$$

And rearranging

$$-\frac{3r}{r-1} f_o = p \frac{df_o}{dp} + \frac{3r}{r-1} \frac{\eta n_1}{4\pi p_{inj}^2} \delta(p - p_{inj})$$

when $p \neq p_{inj}$, the equation is

$$-\frac{3r}{r-1} f_o = p \frac{df_o}{dp}$$

the solution is

$$f_o(p) = k \left(\frac{p}{p_{inj}} \right)^{-\frac{3r}{r-1}}$$

Imposing the continuity of f at p_{inj} , $f(p_{inj}) = q_0$, we get

$$k = \frac{3r}{r-1} \frac{\eta n_1}{4\pi p_{inj}^2}$$

The diffusion approach

$$f_o(p) = \frac{3r}{r-1} \frac{\eta n_1}{4\pi p_{inj}^2} \left(\frac{p}{p_{inj}} \right)^{-\frac{3r}{r-1}}$$

The slope tends asymptotically to $\alpha = 4$ in the limit $M \rightarrow \infty$ of an infinitely strong shock front.

The number density of particles with energy between E and $E + dE$ is

$$n(E)dE = 4\pi p^2 f_o(p(E)) \frac{dp}{dE} dE$$

For ultrarelativistic particles (UR) $p = E$ and $n(E) \propto E^{\alpha-2}$

For non relativistic particles (NR) $p = (2mE)^{1/2}$ and $n(E) \propto E^{(1-\alpha)/2}$

For strong shocks $\alpha = 4$ and

$$n(E) \propto E^{-2}$$

For UR particles

$$n(E) \propto E^{-3/2}$$

For NR particles

The diffusion approach

$$f_o(p) = \frac{3r}{r-1} \frac{\eta n_1}{4\pi p_{inj}^2} \left(\frac{p}{p_{inj}} \right)^{-\frac{3r}{r-1}}$$

Some points are worth being mentioned: the shape of the spectrum of the accelerated particles does not depend upon the diffusion coefficient. On one hand this is good news, in that the knowledge of the diffusion properties of the particles represent the greatest challenge for any theory of particle acceleration. On the other hand, this implies that the concept of maximum energy of accelerated particles is not naturally embedded in the test particle theory of DSA. In fact, the power law distribution derived above does extend (in principle) contains a divergent energy, thereby implying a failure of the test particle assumption. Clearly the absence of a maximum energy mainly derives from the assumption of stationarity of the acceleration process, which can be achieved only in the presence of effective escape of particles from the accelerator, a point which is directly connected to the issue of maximum energy, as discussed in

SOME IMPORTANT COMMENTS

- 🔗 THE STATIONARY PROBLEM DOES NOT ALLOW TO HAVE A MAX MOMENTUM!
- 🔗 THE NORMALIZATION IS ARBITRARY THEREFORE THERE IS NO CONTROL ON THE AMOUNT OF ENERGY IN CR
- 🔗 AND YET IT HAS BEEN OBTAINED IN THE TEST PARTICLE APPROXIMATION
- 🔗 THE SOLUTION DOES NOT DEPEND ON WHAT IS THE MECHANISM THAT CAUSES PARTICLES TO BOUNCE BACK AND FORTH
- 🔗 FOR STRONG SHOCKS THE SPECTRUM IS UNIVERSAL AND CLOSE TO E^{-2}
- 🔗 IT HAS BEEN IMPLICITELY ASSUMED THAT WHATEVER SCATTERS THE PARTICLES IS AT REST (OR SLOW) IN THE FLUID FRAME

Acceleration time

* see eqn. 3.36

In the assumption of isotropy, the flux of particles that cross the shock from downstream to upstream is $n_s c/4$,* which means that the upstream section is filled through a surface Σ of the shock in one diffusion time upstream with a number of particles $n_s (c/4) \tau_{diff,1} \Sigma$ (n_s is the density of accelerated particles at the shock). This number must equal the total number of particles within a diffusion length upstream $L_1 = D_1/u_1$, namely:

$$n_s \frac{c}{4} \Sigma \tau_{diff,1} = n_s \Sigma \frac{D_1}{u_1}, \quad (45)$$

which implies for the diffusion time upstream $\tau_{diff,1} = \frac{4D_1}{cu_1}$. A similar estimate downstream leads to $\tau_{diff,2} = \frac{4D_2}{cu_2}$, so that the duration of a full cycle across the shock is $\tau_{diff} = \tau_{diff,1} + \tau_{diff,2}$. The acceleration time is now:

$$\tau_{acc} = \frac{E}{\Delta E / \tau_{diff}} = \frac{3}{u_1 - u_2} \left[\frac{D_1}{u_1} + \frac{D_2}{u_2} \right]. \quad (46)$$

Acceleration time

Define a cycle $\equiv U \rightarrow \text{shock} \rightarrow D \rightarrow \text{shock} \rightarrow U$, so $\tau_{\text{acc}} = E/(dE/dt) = \tau_{\text{cycle}}/\xi$. But, $\tau_{\text{cycle}} = ?$

Let t_2 be the average time spent in D before returning to the shock, i.e., for $(S \rightarrow D \rightarrow S)$.

Average distance in D through which particle diffuses in time t is $\approx \sqrt{k_2 t}$, with $k_2 =$ diffusion coefficient in D.

Average distance through which the particle is advected in D in time t is $= u_2 t$.

The particle is lost downstream (i.e., low probability of returning to shock) if $u_2 t > \sqrt{k_2 t}$. Thus, ‘returning zone boundary’ is given by the condition $u_2 t \approx \sqrt{k_2 t}$. Thus only the particles within a distance $d_2 \approx \frac{k_2}{u_2}$ from the shock return to the shock.

Number of particles per unit area within the ‘returning zone’ is $n_{\text{CR}} d_2 = n_{\text{CR}} \frac{k_2}{u_2}$. Thus,

$$t_2 \approx n_{\text{CR}} d_2 / r_{\text{cross}}, \text{ i.e., } t_2 = \frac{4 k_2}{c u_2}.$$

Similarly, for $S \rightarrow U \rightarrow S$, we have $t_1 = \frac{4 k_1}{c u_1}$. Thus, $\tau_{\text{cycle}} = \frac{4}{c} \left(\frac{k_1}{u_1} + \frac{k_2}{u_2} \right)$.

$$\text{Thus, } r_{\text{acc}} = \frac{R-1}{3R} u_1 \left(\frac{k_1}{u_1} + \frac{k_2}{u_2} \right)^{-1}.$$

Note that the higher is the diffusion, the longer is the acceleration time

A CRUCIAL ISSUE: the maximum energy of accelerated particles

1. The maximum energy is determined in general by the balance between the Acceleration time and the shortest between the lifetime of the shock and the loss time of particles
2. For the ISM, the diffusion coefficient derived from propagation is roughly

$$D(E) = 3 \times 10^{29} E_{GeV}^{\alpha} \quad \alpha \approx 0.3 - 0.6$$

$$\tau_{acc}(E) = \frac{3}{u_1 - u_2} \left[\frac{D_1(E)}{u_1} + \frac{D_2(E)}{u_2} \right]$$

For a typical SNR the maximum energy comes out as FRACTIONS OF GeV !!!



Particle Acceleration at Parallel Collisionless Shocks works ONLY if there is additional magnetic scattering close to the shock surface that makes the diffusion slow

Acceleration time

- Energy gain at each crossing : $\Delta E = \frac{v_1}{c} E$ if $r = 4$.
- What is the duration of cycle ?
- It depends on particle isotropization timescale
- We introduce the diffusion coefficient D in $m^2.s^{-1}$
- During time t , particle diffuse in its medium on a typical length :

$$l_d = \sqrt{Dt}$$

- In the meantime, the shock has moved on a distance : $l_s = vt$
- Equating the two length give the residence timescale :

$$t = \frac{D}{v^2}$$

Acceleration time

$$\langle \Delta t_{cycle}(E) \rangle = 4 \left(\frac{D_1(E)}{v_1 c} + \frac{D_2(E)}{v_2 c} \right) \quad (3.46)$$

where D_1 and D_2 are the diffusion coefficients for the upstream and downstream media respectively. Then for the acceleration time we have :

$$\langle t_{acc}(E) \rangle = \frac{\langle \Delta t_{cycle}(E) \rangle}{\langle \frac{\Delta E}{E} \rangle} \propto \frac{D(E)}{v_{sh}^2} \quad (3.47)$$

The energy dependence of the acceleration time is then given by the energy dependence of the diffusion coefficient which is related to the type of magnetic turbulence. As we saw in Chapt. 2 that for a Kolmogorov turbulence, in the limit $r_L(E) \ll \lambda_{max}$ we have $D(E) \propto E^{1/3}$. We will make a different assumption in the following mostly for the sake of simplicity. $D(R) = \lambda(R) c \beta / 3$

Indeed, in most calculation, the *Bohm scaling* (or Bohm approximation) is usually assumed for the energy evolution of the diffusion coefficient. In the general case : $D(E) = \frac{1}{3} l_{scat} v$ where l_{scat} is the scattering length (or mean free path), *i.e* the length on which the particle get "randomized" and losses the memory of its initial direction and v is the velocity of the particle. The Bohm diffusion coefficient is obtained by assuming $l_{scat}(R) = r_L(E)$, where $r_L = \frac{P}{ZeB} = \frac{R}{Bc}$ is the Larmor radius of a particle of momentum P and rigidity R (see Chapt. 2). We then have,

$$D_{Bohm}(R) = \frac{1}{3} r_L(R) c \quad (3.48)$$

Acceleration time

With the Bohm hypothesis, we then get :

$$\langle t_{acc}(R) \rangle \propto \frac{R}{B} \times \frac{1}{v_{sh}^2} \quad (3.49)$$

(a dependence in $R^{1/3}$ would be expected for a Kolmogorov turbulence).

Before going further we can obtain some useful scaling laws (the reader is invited to recalculate them) :

$$r_L(R) \simeq 1.1 \times \left(\frac{R}{10^{15} \text{V}} \right) \times \left(\frac{B}{\mu\text{G}} \right)^{-1} \text{ pc} \quad (3.50)$$

$$D_{Bohm}(R) \simeq 3.4 \times 10^{28} \times \left(\frac{R}{10^{15} \text{V}} \right) \times \left(\frac{B}{\mu\text{G}} \right)^{-1} \text{ cm}^2 \text{ s}^{-1} \quad (3.51)$$

Let us now quantify a little our finding using typical parameters probably at play in a supernova remnant. We remind that *supernova remnants* are what remains of a supernova hundreds to tens of thousands of years after a supernova explosion. The phenomenon is explained by the propagation of a supersonic plasma, emitted at the time of the supernova event, through the interstellar medium. The shock wave is known to heat up the shocked interstellar medium and to accelerate electrons and nuclei which emit non thermal radiation up to very high energies. Supernova remnants are considered as one of the best source candidate for the acceleration of Galactic cosmic-rays⁸. The

The physical parameters which are important to discuss CR acceleration by supernova remnant evolve with time⁹, we will limit ourselves for the type being to typical values thought to be at play in the vicinity of the shock wave a few hundred years after the supernova explosion.

The typical value of the magnetic field and the shock velocity is thought to vary from remnants to remnants $B \sim [100, 500] \mu\text{G}$, $v_{sh} \sim [1000, 10000] \text{ km s}^{-1}$. Let us use $B = 100 \mu\text{G}$ and $v_{sh} = 3000 \text{ km s}^{-1}$ as typical values. For a proton at 100 GeV we have $D_{Bohm}(100\text{GeV}) \simeq 3.4 \times 10^{22} \text{ cm}^2 \text{ s}^{-1}$. Thus,

$$\langle \Delta t_{cycle} \rangle_{100 \text{ GeV}} \simeq \frac{4D(E)}{cv_{sh}} \simeq 1.5 \cdot 10^4 \text{ s} \quad (3.52)$$

$$\langle t_{acc} \rangle_{100 \text{ GeV}} = \frac{\langle \Delta t_{cycle} \rangle_{100 \text{ GeV}}}{\langle \frac{\Delta E}{E} \rangle} \simeq \frac{4D(E)}{v_{sh}^2} \simeq 1.5 \cdot 10^6 \text{ s} \simeq 17.5 \text{ days} \quad (3.53)$$

Using $t_{acc}(E) \propto E$ (assuming Bohm scaling) we get :

$$\langle t_{acc} \rangle_{10^{15} \text{ eV}} \simeq 480 \text{ years} \quad (3.54)$$

Although the discussion of cosmic-ray acceleration in supernova remnants goes of course far beyond the order of magnitude calculation we just made, we can use our results to compare with what we obtained for the second order Fermi mechanism we discussed in the previous section. The comparison speaks for itself. With DSA we now get much more reasonable acceleration times which can be achieved within the source lifetime (see next chapter for a more complete (although oversimplified) discussion) and which can also compete with energy loss mechanisms.

Acceleration time

- The diffusion distance upstream of the shock is then :

$$l_d = \frac{D_1}{v_1}$$

- It is possible to show that the duration of a cycle is :

$$\tau_{acc} = \frac{4}{c} \left(\frac{D_1}{v_1} + \frac{D_2}{v_2} \right)$$

- We use in general the Bohm diffusion coefficient

$$D = \frac{pc}{3ZeB}$$

- Then assuming $D_1 = D_2$, we have

$$\tau_{acc} = \frac{4(r+1)E}{3ZeBv_1c} \propto E$$

- The energy gain rate is then :

$$\frac{dE}{dt} = \frac{\Delta E}{\tau_{acc}} = \frac{r-1}{r(r+1)} ZeBv_1^2$$

Acceleration time

- For a typical young supernova remnant shock :
 $v_1 \sim 10^4 \text{ km/s}$ and $B = 2nT$:

$$\frac{dE}{dt} \sim 30 \text{ keV/s} \left(\frac{v}{10^4 \text{ km/s}} \right)^2 \left(\frac{B}{2nT} \right)$$

- To reach 100 TeV, only ~ 100 yrs are necessary.
- **Efficient acceleration mechanism !**
- E_{max} is limited by several factors :
 - Energy losses (Coulomb, radiative, inelastic collisions)
 - Time : age of the system limits the energy
 - Particle escape (geometry effect)
- Maximal energy depends of system physical conditions

Particle confinement and maximum achievable energy

At this stage, it is useful to discuss some of the assumptions we made to calculate the accelerated particle spectrum, *i.e.* infinite media (upstream and downstream) and steady conditions (shock lasting forever).

In any astrophysical source, the acceleration region has in principle a finite spatial extension (and of course a finite age and activity duration) and as a consequence, the Larmor radius of the accelerated particles cannot exceed the size of the acceleration site.

Taking for instance $B = 100 \mu G$ and $L_{source} = 1 \text{ pc}$, one can estimate a maximum energy E_{max}^{size} such that $r_L(E_{max}^{size}) = L_{source}$. With these parameters, one gets $E_{max}^{size} \simeq Z \times 10^{17} \text{ eV}$ or in terms of the maximum rigidity $R_{max}^{size} \simeq 10^{17} \text{ V}$.

Particle confinement and maximum achievable energy

An argument very close to that one was used by M. Hillas (in 1984) to build the famous *Hillas diagram* estimating the maximum energy achievable for cosmic-rays in different types of sources as a function of their size and their ambient magnetic field. Hillas constructed his famous diagram in order to select viable sources for cosmic-ray acceleration above 10^{20} eV, a version of it is visible in Fig. 3.10. We must note that the "Hillas condition" is a necessary but not sufficient condition to estimate whether or not a given energy can be achieved in a given type of source. In most cases as we will discuss later the maximum energy estimated with this criterion is overoptimistic. Moreover energy losses, which may limit the acceleration process (see next chapter) and which are specific to a given type of source, are not accounted for in this argument.

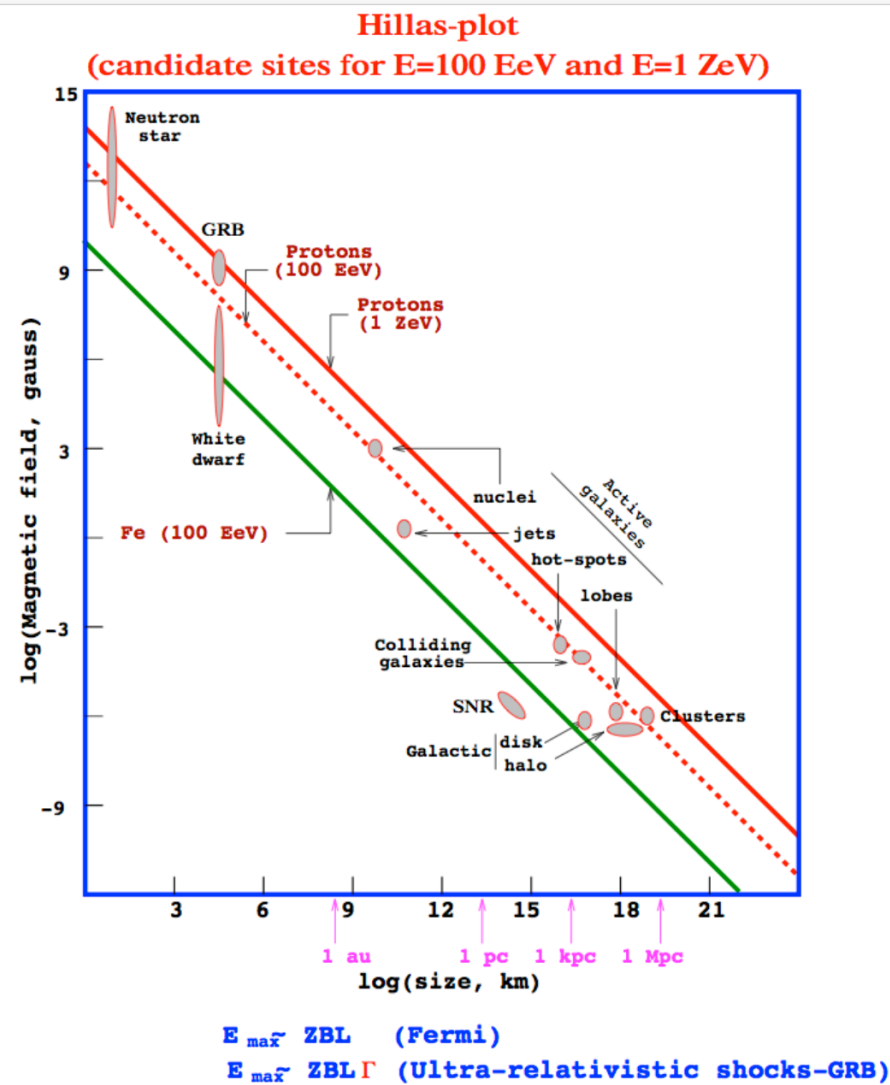


FIG. 3.10: Hillas diagram constructed by plotting different sources characteristics in the (size, B) plane. Sources above the green line may be able to accelerate Fe nuclei above 10^{20} eV, while those above the dashed and full red lines may be able to accelerate protons above 10^{20} and 10^{21} eV respectively. Note that the Hillas must be interpreted with the greatest caution : (i) The Hillas criterion is a necessary but not sufficiently condition to reach a given maximum energy. (ii) The maximum energies estimated using the Hillas criterion are overoptimistic (see text). (iii) Energy losses during the acceleration process (which may limit the maximum reachable energy) are not taken into account.

Particle confinement and maximum achievable energy

A slightly higher level argument can be used to derive a more quantitative estimate. In diffusion theory, one can show that the typical distance from the shock a particle manages to reach upstream or downstream and which is called the diffusion length is given by :

$$L_{diff} \simeq \frac{D(E)}{v_{sh}} \quad (3.55)$$

when the value of L_{diff} reaches a value of the order of the spatial extension of the magnetized region upstream of the shock then particle escape in the upstream region becomes efficient (and the approximation we made for our calculation is broken). We can then define a maximum energy due to particle confinement E_{max}^{conf} such that $L_{diff}(E_{max}^{conf}) = L_{up}$, where L_{up} is the size of the magnetized region upstream of the shock. Since particles with energy of the order of E_{max}^{conf} will escape efficiently upstream rather than re-crossing the shock, this escape mechanism is going to limit the maximum energy achievable by cosmic-rays which was not the case in our idealized calculation. This is however a good thing since the particles escaping downstream of the shock were not accelerated anymore but were still trapped within the source without any possibility to escape through the interstellar medium until the phenomenon at the origin of the acceleration dissipates. These particles would be likely to experience energy losses while being confined in the source. Particles escaping upstream by de-confinement eventually escape through the interstellar medium and can propagate throughout the Galaxy.

Particle confinement and maximum achievable energy

Particles with energies close to E_{max}^{conf} can escape efficiently upstream while at much lower energy the probability for reaching the boundary of the magnetized region upstream of the shock is very low¹⁰. For these low energy particles the above approximation of an infinite spatial extension for the upstream medium is relatively accurate.

$$L_{diff}(R) \simeq 110 \times \left(\frac{R}{10^{15} \text{V}} \right) \times \left(\frac{B}{\mu\text{G}} \right)^{-1} \times \left(\frac{v_{sh}}{1000 \text{ km s}^{-1}} \right)^{-1} \text{ pc} \quad (3.56)$$

Using the same supernova remnant parameters as before and assuming $L_{up} = 0.1 \text{ pc}$ (the size of the upstream magnetised region is often assumed to be of the order of 1/10th of the size of remnant for which we use $L_{source} = 1 \text{ pc}$). We get $E_{max}^{conf} \simeq Z \times 3 \cdot 10^{14} \text{ eV}$ (or $R_{max}^{conf} \simeq 3 \cdot 10^{14} \text{ V}$) which is indeed much smaller than the above calculated E_{max}^{size} .

The important thing to understand here is that particles escaping upstream are directly released in the ISM and will eventually propagate through the Galaxy. They are the cosmic-rays we expect to detect on Earth. Since only particles with rigidities close to R_{max}^{conf} have a significant probability to escape upstream by reaching the boundary of the magnetized region, the spectrum of particles escaping upstream is expected to be much harder than the spectrum of accelerated cosmic-rays (one might call this phenomenon a "high pass filter effect"). This very important fact is illustrated in Fig. 3.11.

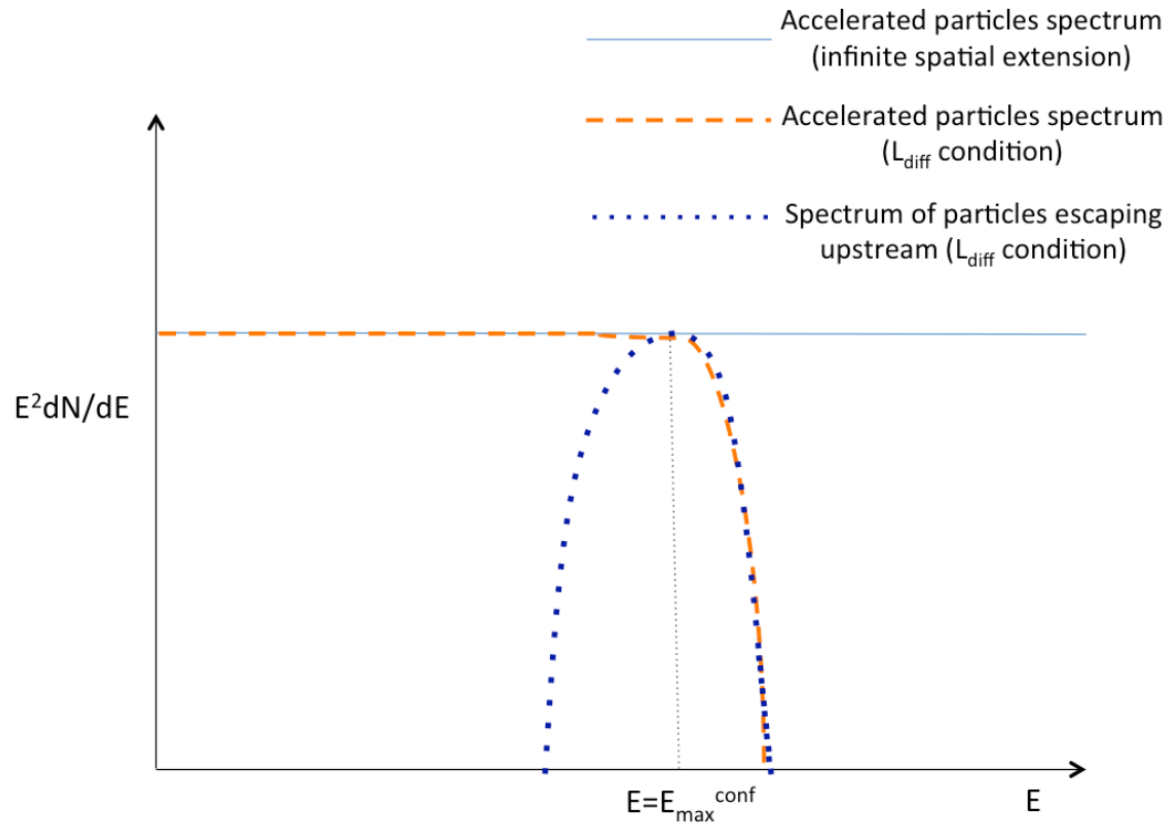


FIG. 3.11: Schematic view explaining the impact of the existence of the diffusion length and the limited confinement capabilities of a source : When the spatial extension of the source is assumed to be infinite, the spectrum of the accelerated cosmic-rays is proportional to E^{-2} and can reach arbitrarily large energies (blue line). When the spatial extension of the source is considered (and the condition on $L_{diff}(R)$ applied), the spectrum of the accelerated cosmic-rays is still proportional to E^{-2} but the acceleration mechanism becomes inefficient above E_{max}^{conf} since particles start to escape upstream of the shock rather than coming back to the shock and starting a new cycle (orange dashed line). Finally the dark blue dotted line shows the spectrum of particles which manage to escape upstream of the shock. The spectrum is very hard (almost a Dirac distribution) since the escape probability only becomes significant for energies close to E_{max}^{conf} . Above this energy the efficient escape upstream prevent the particles from performing extra cycles and reaching higher energies.

Age limit

Another source of limitation for the acceleration of cosmic-rays might come from the "age" of the source (in other word the amount of time during which the source has been active). This criterion

is relatively straightforward to understand : if a source has an age t_{source} then only the rigidities for with $t_{acc}(R) \leq t_{source}$ can be potentially reached.

For instance, we saw earlier that $\langle t_{acc}(10^{15} \text{ V}) \rangle \simeq 480 \text{ yr}$. Thus for an SNR with $B = 100 \mu\text{G}$ and $v_{sh} = 3000 \text{ km s}^{-1}$ the maximum rigidity due to the age of the source after 480 yr will be $R_{max}^{age} \simeq 10^{15} \text{ V}$. Since in the Bohm hypothesis, $\langle t_{acc}(R) \propto R \rangle$ then if v_{sh} and B were constant with time, we would expect $R_{max}^{age} \propto t$.

Age Limit

Let us now discuss the comparison between R_{max}^{age} and R_{max}^{conf} , assuming for the time being v_{sh} and B are constant with time. After 480 yr, we have $L_{source} = v_{sh} \times t \simeq 1.45$ pc. Let us take $L_{up} \simeq 0.1 L_{source} \simeq 0.145$ pc. Then we would get with the same calculation as above $R_{max}^{conf}(480 \text{ yr}) \simeq 5 \cdot 10^{14}$ V. Then at $t = 480$ yr we have $R_{max}^{conf} \simeq R_{max}^{age}$ (within a factor of 2) and it should remain so at least while v_{sh} and B are constant (in which case as we saw $R_{max}^{age} \propto t$ and moreover $L_{up} \propto L_{source} \propto t \Rightarrow R_{max}^{conf} \propto t$).

In this situation the escape of particles becomes efficient at a rigidity which is practically the same as the maximum rigidity the cosmic accelerator can achieve (due to its age). This is actually a quite optimum situation and we can understand this point by considering two extreme cases :

(i) if $R_{max}^{conf} \gg R_{max}^{age}$, in this case, the escape of particles at the maximum energy achievable is inefficient and then the accelerated particles remain trapped in the source.

(ii) if $R_{max}^{conf} \ll R_{max}^{age}$, in this case, particle escape becomes efficient at rigidities much lower than the maximum energy the source could achieve. This efficient escape would "break" the acceleration mechanism (see above) before reaching the rigidity R_{max}^{age} .

The case $R_{max}^{conf} \simeq R_{max}^{age}$ is then optimum since the criteria for an efficient particle escape upstream and for the acceleration of the particles to the maximum possible energy due to the age of the source are met at the same time.

Maximum energy : age limit

- Maximal energy of a particle in an accelerator for time t
- Using the acceleration rate :

$$E_{max} = \int_0^t \frac{dE}{dt} dt = \int_0^t \frac{r-1}{r(r+1)} Z e B V_s^2 dt$$

- If we assume the shock velocity is constant

$$E_{max,age} = \frac{r-1}{r(r+1)} Z e B V_s^2 t$$

- Or for $r = 4$ and parameters typical of a supernova remnant :

$$E_{max,age} \sim 12 TeV \left(\frac{B}{1 nT} \right) \left(\frac{V_s}{5 \cdot 10^3 km/s} \right)^2 \left(\frac{t}{100 yrs} \right)$$

Maximum energy : radiative limit

- For an electron radiative losses oppose acceleration

$$\frac{dE}{dt} = -bU^2 E^2 \quad \text{with } U = B^2/2\mu_0$$

- Radiative limit**

- E_{max} is reached when $\dot{E}_{acc} + \dot{E}_{rad} = 0$
- Using t_{acc} :

$$\dot{E}_{acc} = bU_B E_{max}^2 \Rightarrow E_{max} = \left(\frac{\dot{E}_{acc}}{bU} \right)^{1/2}$$

$$E_{max,rad} = \left(\frac{3}{2} \frac{r-1}{r(r+1)} \frac{e\mu_0}{\sigma_T c B} \right)^{1/2} V_s m_e c^2$$

- For a typical SNR :

$$E_{max,rad} = 240 \text{ TeV} \left(\frac{V_s}{10^4 \text{ km/s}} \right) \left(\frac{B}{1 \text{ nT}} \right)^{-1/2}$$

Maximum energy : size limit

- If the shock is not an infinite plane, the particle diffusing far upstream won't be caught up
- E.g. : a SNR has a spherical shape of radius R
 - Particle distribution upstream : $n(x) = n_0 e^{-V_c/D x}$
 - Characteristic length $l = \frac{D}{u}$
 - Escape if $l \geq \eta R_c$ that is using the Bohm limit ($\lambda_{diff} = r_g$) :

NB: typo $R_c = R_s$, $V_{sc} = V_s$

$$D = \frac{p c}{3 Z e B} = \eta V_{sc} R_s \Rightarrow E_{max, size} = 3 Z e B \eta V_s R_s$$

with $\eta \leq 1$ a factor controlling the escape probability

- In the adiabatic evolution phase : $R_c = R_{ST} t^{2/5}$ and $V_c = V_{ST} t^{-3/5}$

$$E_{max, size} = 3 Z e \eta B V_{ST} R_{ST} t^{-1/5}$$

$$E_{max, taille} = 125 \text{ TeV } Z \left(\frac{\eta}{0.2} \right) \left(\frac{E}{10^{44} \text{ J}} \right)^{\frac{2}{5}} \left(\frac{n_0}{10^6 \text{ m}^{-3}} \right)^{-\frac{2}{5}} \left(\frac{t}{10^3 \text{ ans}} \right)^{-1}$$

SNR : maximum energies

- Maximum energy grows with time until t so that

$$E_{max} = E_{max,size}(t) = E_{max,age}(t)$$

- This limit is typically of the order of

$$E_{max} \approx 120 \text{ TeV } Z \left(\frac{B}{1 \text{ nT}} \right)$$

- **With typical B fields, Supernova Remnants can't accelerate up to the knee ($3 \cdot 10^{15}$ eV)!**
- Once this limit is reached, the most energetic particles escape slowly ($E_{max} \propto t^{-1/5}$)
- Electrons are very quickly limited by radiative losses
- The higher B , the lower $E_{max,e}$
- **The highest energy particles escape slowly the SNR shock : efficient acceleration for a limited period of time**

Toy model of the time evolution of a SNR

As mentioned in the previous chapter, the SNR phenomenon is caused by the ejection of a supersonic plasma (or wind) at the time of the supernova event. The supersonic flow propagates in the surrounding ISM, the gas swept by the shock is both compressed and heated (see Eqs. 3.21 to 3.28) and particles are expected to be accelerated by the DSA mechanism. The flow propagates until it becomes subsonic and eventually mixes with the ISM, the whole process lasts in total up to 10^5 years. From the point of view of particles acceleration a SNR probably remain efficient during $\sim 10^4$ years or so. During this period of time there are mainly two phases in the shock propagation

Toy model of the time evolution of a SNR

(i) The free expansion phase which lasts a few hundreds of years in general (depending on the characteristics of the wind and of the surrounding ISM). During the phase, the shock velocity v_{sh} is in good approximation constant which means that the shock radius R_{sh} is proportional to the elapsed time, $R_{sh} \propto t$. The time evolution of the magnetic field in the vicinity of the shock is not precisely known while it is of course a quantity of major importance for particle acceleration. We will assume in the following that the shock magnetic field B remains constant during the free expansion phase (i.e, proportional to v_{sh}). It is however important to note that scenarios involving very strong magnetic fields at the very early times of the shock propagation are currently extensively studied¹.

¹These scenarios are relatively attractive since (as we will discuss later) there is no signature of the acceleration of cosmic-rays up to the knee energy in the photon spectra of the SNRs observed in γ -rays. Since those SNRs are all more than 100 years old, it can be invoked that those SNRs are not able anymore to accelerate cosmic-rays up to the knee energy but that they were earlier in their evolution. The scenario we will discuss in the following is different since we will assume B is constant during the free expansion phase.

Explosion and free expansion phase

- Kinetic energy released during Supernova explosion
 $E_k \sim 10^{44} \text{ J}$
- Sphere of ejected matter (total mass M_{ej}) expanding in a uniform density medium.
- At the shock itself, V_s is constant (no energy loss). The shock radius is then $R_s = V_s t$.
- The total kinetic energy is :

$$E_k \sim \frac{1}{2} M_{ej} V_s^2$$

- For an explosion of $E_k = 10^{44} \text{ J}$ with $M_{ej} = 1 M_\odot$

$$V_s = \sqrt{2 \frac{E_c}{M_{ej}}} = 10000 \text{ km/s} \left(\frac{E_c}{10^{44} \text{ J}} \right)^{1/2} \left(\frac{M_{ej}}{1 M_\odot} \right)^{-1/2}$$

- **In the early phases after the explosion the shock speed can be as large as $0.03c$!**

(ii) The Sedov-Taylor phase : after a few hundreds of years, once the shock has swept a mass of ISM greater or equivalent to its own, the shock starts to decelerate. During the Sedov-Taylor phase the velocity of the shock radius is expected to scale as $R_{sh} \propto t^{2/5}$ and then $v_{sh} \propto t^{-3/5}$. We will not discuss in detail the implications of the Sedov-Taylor phase for the SNR gas dynamics but just the aspects of the evolution which are relevant for particle acceleration within our simplified model, the interested reader can find many more details in the chapter 16 of M. Longair's book, "*High Energy Astrophysics*". The Sedov-Taylor scaling is a standard result of fluid dynamics obtained by dimensional analysis (see M. Longair's book "*Theoretical Concepts in Physics*") and experimentally observed in the behavior of shock waves produced by nuclear explosions². The evolution of the magnetic field during this phase is not well known, we will assume, as in the free expansion phase that the magnetic field is proportional to the shock velocity³, $B \propto v_{sh}$.

Transition to the Sedov-Taylor phase

- When the ejected mass is equal to the mass of the swept up interstellar matter, hydrodynamic evolution changes. SNR is now an adiabatic phase where the evolution is guided by the initial kinetic energy and the mass of the swept up matter
- Temperatures are very large (so $T > 10^8$ K) so that radiative cooling of the thermal energy is inefficient and evolution is adiabatic
- Transition when :

$$\frac{4}{3}\pi R_s^3 \rho_0 = \frac{4}{3}\pi v_s^3 t^3 \rho_0 = M_{ej}$$

- That is :

$$t_{ST} = 120 \text{ yrs} \left(\frac{E}{10^{44} \text{ J}} \right)^{-\frac{1}{2}} \left(\frac{n_0}{10^6 \text{ m}^{-3}} \right)^{-\frac{1}{3}} \left(\frac{M_{ej}}{1 M_{\odot}} \right)^{\frac{5}{6}}$$

$$R_{ST} = 2.2 \text{ pc} \left(\frac{n_0}{10^6 \text{ m}^{-3}} \right)^{-\frac{1}{3}} \left(\frac{M_{ej}}{1 M_{\odot}} \right)^{\frac{1}{3}}$$

Sedov-Taylor phase

An autosimilar solution allows to describe the adiabatic evolution of an expanding shock wave.

Simply, if we assume that a constant fraction of the energy is in the form of kinetic energy

$$\rho R^3 V^2 = \text{const}$$

$$R^{3/2} \frac{dR}{dt} = \text{const}$$

Therefore

$$R^{5/2} \propto t \quad \text{and} \quad R \propto t^{2/5} \quad V \propto t^{-3/5}$$

Let us assume, for our toy model, that the initial velocity of the shock is $v_{sh} = 3000 \text{ km s}^{-1}$, the magnetic field $B = 100 \text{ } \mu\text{G}$ and that the free expansion phase lasts for 480 years before entering in the Sedov-Taylor phase⁴. Under these assumptions, the time evolution of R_{sh} and v_{sh} are represented in Fig. 4.1.

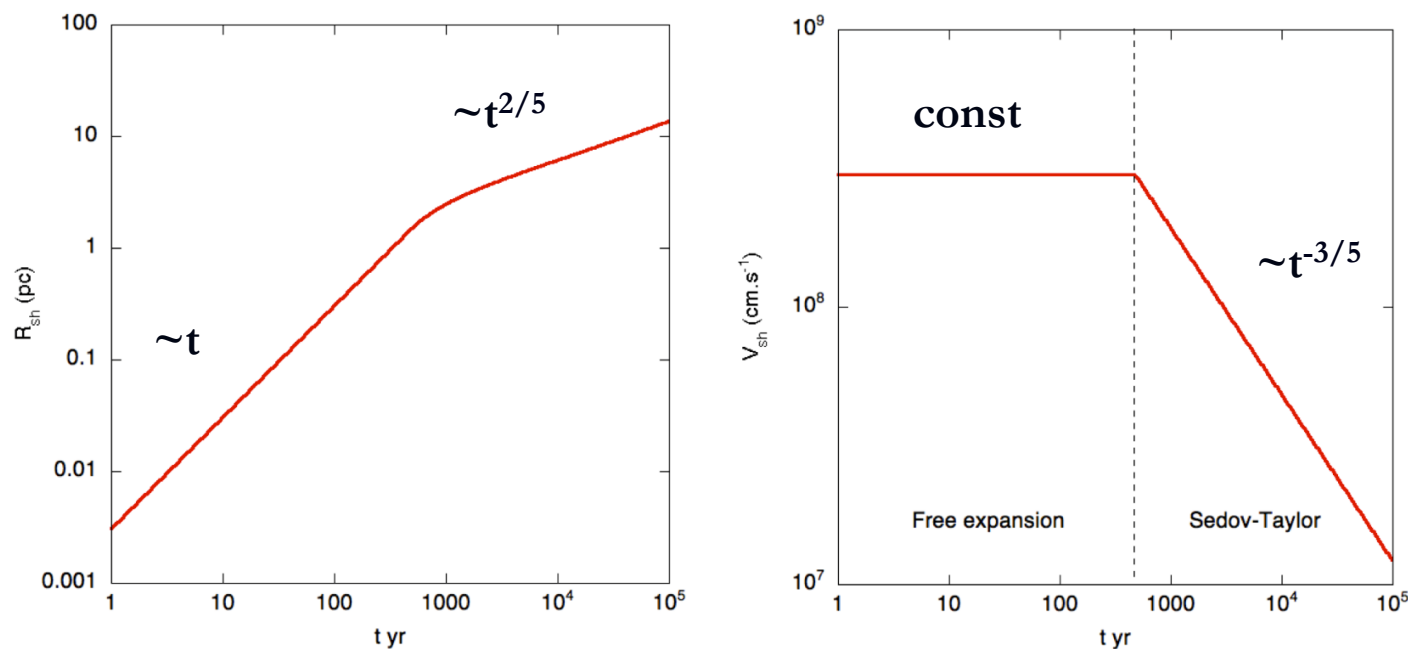


FIG. 4.1: Time evolution of r_{sh} (left) and v_{sh} for our SNR toy model parameters (see text).

Free expansion phase

From our discussions in the last paragraph of Chapt. 3, we already know the evolution of R_{max}^{conf} and R_{max}^{age} in the free expansion phase. We know that $R_{max}^{age}(480 \text{ yr}) \simeq 10^{15} \text{ V}$ and $R_{max}^{conf}(480 \text{ yr}) \simeq 5 \cdot 10^{14} \text{ V}$. Since we are assuming the Bohm scaling for the rigidity evolution of the diffusion coefficient and as a result that $t_{acc}(R) \propto R$ then we get $R_{max}^{age} \propto t$. On the other hand since $v_{sh} = \text{cst}$ and then

$R_{sh} \propto t$, with our assumption of $L_{up} \simeq 0.1 R_{sh}$ (see the last paragraph of the previous chapter) then we have $L_{up} \propto t$ which gives (still due to the Bohm scaling assumption with yields $L_{diff}(R) \propto R$) $R_{max}^{conf} \propto t$. We can deduce the time evolution of R_{max}^{age} and R_{max}^{conf} during the free expansion phase, for our choice of physical parameters :

$$R_{max}^{age} \simeq 10^{15} \left(\frac{t}{480 \text{ yr}} \right) \text{ V for } t \leq 480 \text{ yr} \quad (4.1)$$

and

$$R_{max}^{conf} \simeq 5 \cdot 10^{14} \left(\frac{t}{480 \text{ yr}} \right) \text{ V for } t \leq 480 \text{ yr} \quad (4.2)$$

Sedov-Taylor phase

The time evolution of the different maximum rigidities can be calculated very simply from the definitions of R_{max}^{conf} and R_{max}^{age} .

R_{max}^{age} is such that $t_{acc}(R_{max}^{age}) = t_{source}$. Since,

$$t_{acc}(R) \simeq \frac{4D(R)}{v_{sh}^2} \propto \frac{R}{Bv_{sh}^2} \text{ then } R_{max}^{age} \propto tBv_{sh}^2 \propto tt^{-3/5}t^{-6/5} \propto t^{-4/5} \quad (4.3)$$

using the assumed Bohm scaling of the diffusion coefficient, the scaling with time of v_{sh} during the Sedov-Taylor phase and our assumption on the magnetic field evolution.

On the other hand, R_{max}^{conf} is such that $L_{diff}(R_{max}^{conf}) = L_{up} \simeq 0.1R_{sh}$. Since,

$$L_{diff}(R) \simeq \frac{D(R)}{v_{sh}} \propto \frac{R}{Bv_{sh}} \text{ then } R_{max}^{conf} \propto R_{sh}Bv_{sh} \propto t^{2/5}t^{-3/5}t^{-3/5} \propto t^{-4/5} \quad (4.4)$$

(try to redo this reasoning assuming for instance that the magnetic field is constant, or using $D(R) \propto R^{1/3}$ rather than the Bohm scaling)

Sedov-Taylor phase

We then get during the Sedov-Taylor phase we then have

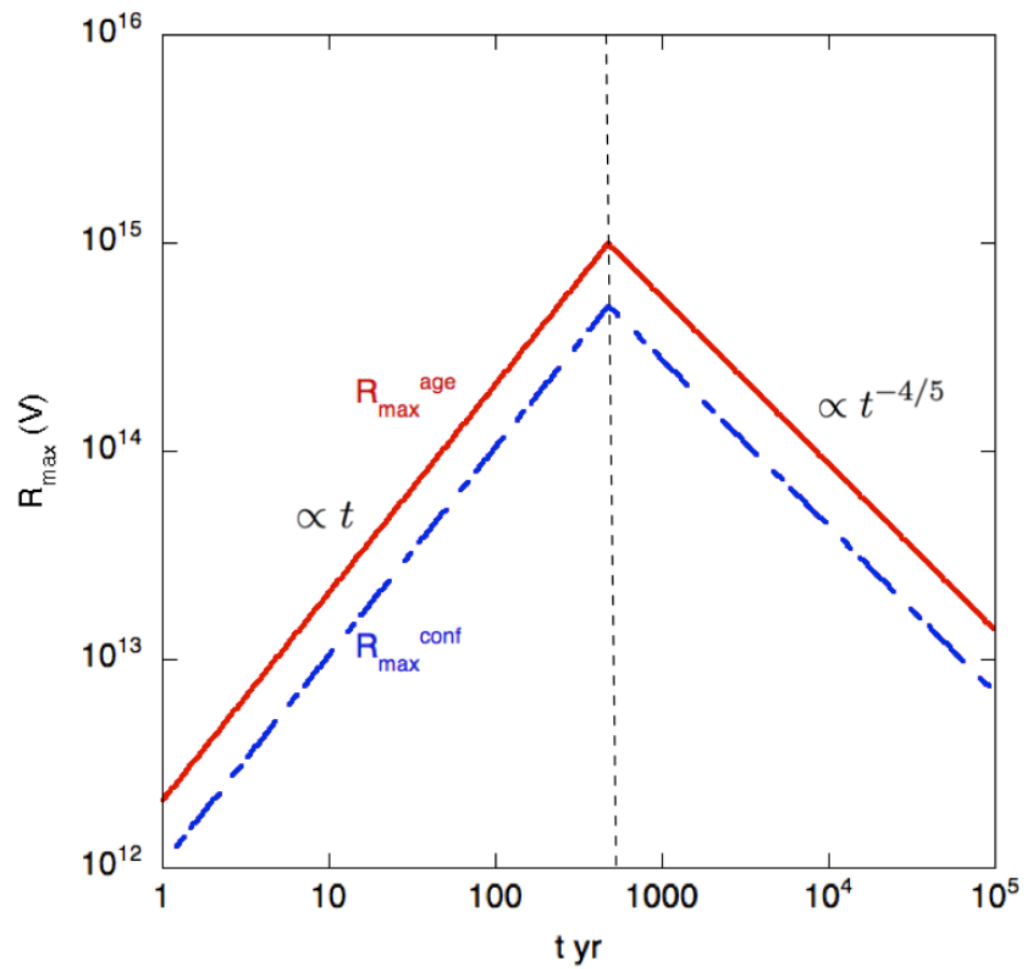
$$R_{max}^{age} \simeq 10^{15} \left(\frac{t}{480 \text{ yr}} \right)^{-4/5} \text{ V for } t > 480 \text{ yr} \quad (4.5)$$

and

$$R_{max}^{conf} \simeq 5 \cdot 10^{14} \left(\frac{t}{480 \text{ yr}} \right)^{-4/5} \text{ V for } t > 480 \text{ yr} \quad (4.6)$$

We see that, within the assumptions of our toy model⁵, R_{max}^{age} and R_{max}^{conf} evolve the same way time (see Fig. 4.2). As a result, as far the escape of cosmic-rays into the ISM is concerned the discussion we had at the of the previous chapter remains true during the whole shock propagation which means that during the whole shock propagation in the ISM, cosmic-rays with rigidities close to $R_{max}^{age}(t)$ escape efficiently from the source. The value of the maximum achievable rigidity increases during the free expansion phase reaching its maximum value before decreasing during the Sedov-Taylor phase as illustrated in Fig. 4.2.

⁵Let us stress again that the evolution we found is only true for the set of simplifying assumptions we made : Bohm scaling, $B \propto v_{sh}$. The scaling with time would be different had we assumed B constant during the whole evolution for instance.



At different times of the shock propagation, the spectrum of escaping cosmic-rays looks like the one displayed in Fig. 3.11, relatively hard and narrow. The instantaneous spectrum of escaping cosmic-rays is then very different (much harder) from the spectrum of the accelerated cosmic-rays ($\propto E^{-2}$ we obtained with the DSA mechanism in the previous chapter. More importantly, it is also very different from the source spectrum which is deduced from the energy evolution of the abundance of LiBeB elements (see Chapt. 2 and Eqs. 2.17 and 2.22, $n(R) = q(R)\tau_{esc}(R) \propto R^{-(\alpha+\beta)}$ with $\alpha = 0.3 - 0.6$ index of the rigidity evolution of the cosmic-ray confinement time in the Galaxy and $\beta = 2.1 - 2.4$ spectral index at the sources). It makes however more sense to compare the source spectral index ($\beta = 2.1 - 2.4$, obtained from cosmic-ray composition measurements) with the spectrum of escaping cosmic-rays integrated over the whole time evolution of the SNR. Indeed, in the hypothesis that SNRs are the main sources of Galactic cosmic-rays then the cosmic-ray spectrum we observe today on Earth would be the sum of the contribution of many different SNR of different age and since the cosmic-ray propagation is diffusive, it is also possible that at a given observation time we could receive cosmic-rays coming from a same SNR but which have escaped at very different epochs of the SNR evolution.

Different studies either numerical or analytic have been performed in order to estimate the time integrated spectrum of cosmic-rays escaping from a SNR. Although these calculations unavoidably rely on assumptions and simplifications it seems that it is possible for the time integrated spectra of escaping cosmic-rays to be compatible with what is required (*i.e* a spectral index $\beta = 2.1$) to make the SNR hypothesis compatible with observations. In any case, we see that, the discussion of the spectrum of cosmic-ray emitted by their possible source goes way beyond the apparent simplicity and universality of the spectrum of accelerated cosmic-ray obtained deriving the DSA mechanism.

Non trivial issues

In this paragraph we will discuss/mention some considerations which go beyond the simple model of the diffusive shock acceleration we derived in the previous chapter but are relevant for the discussion of the origin of Galactic cosmic-ray. Since these discussions make use of relatively advanced notions we will limit ourselves to a very brief discussion.

(i) In the previous chapter, in the version of the DSA mechanism we derived, we neglected the back reaction of the accelerated cosmic-rays on the shock. Such a back reaction is expected to take place when the fraction of the total energy available which is communicated to cosmic-rays is significant (which is supposedly the case in SNRs). In this case, the pressure due to cosmic-rays is expected to modify the physical conditions at play in the vicinity of the shock. Deviations with respect to the universal spectral index $x = 2$ are expected. This issue is currently matter of intense activity in the community. As non linear theories of CR acceleration

Non trivial issues

(ii) Particles injection : As briefly mentioned in the previous chapter, astrophysical shocks are "collisionless" (or non-collisional) and all the energy dissipation at the shock occurs by interactions between the magnetic turbulence carried by the shock and the ambient charged particles. The associated microphysics is beyond the scope of this course, let us note however, that the shock thickness is expected to be of the order of a few Larmor radii of the ambient thermal ions (which carry a lot more momentum than the ambient thermal electrons). To be accelerated, particles must see the shock as a discontinuity which implies that particles must have a Larmor radius initially significantly larger than the shock radius. This condition is in principle fulfilled by ions which are in the high energy tail of the thermal (Maxwellian) distribution. In the case of electrons, the situation is more complicated since thermal electrons have smaller momentum/rigidity/Larmor radii than thermal ions, the question of the injection of electrons at the shock is then highly non trivial... For that reason, it is usually thought that accelerated electrons receive much less energy from the shock than the accelerated ions.

Moreover, let us note that the non-trivial question of particle injection at a shock has also some interesting consequences regarding the relative abundances of the different ionic species as we will discuss later.

Energy losses

So far the acceleration mechanisms we presented, as well as the escape of particles, depended only on the rigidity of the particles and the behavior of protons, nuclei and electrons at a given rigidity was expected to be the same. We expect for instance, the maximum energy of accelerated and escaping protons and electrons to be the same and to be proportional to the atomic number Z for nuclei. This "symmetry" between electrons, protons and other ions is expected to be broken by energy losses that the different species experience during their acceleration and escape, be it in a SNR or in any other type of astrophysical source.

An additional limitation to maximum energy reachable is met when $t_{acc}(E) = t_{loss}(E)$, ($t_{loss}(E)$ being the energy loss time due to a given energy loss process or the sum of different loss processes, see below). We use here for the first time the energy rather than the rigidity since we do not expected electrons, protons and nuclei to behave the same way with respect to energy losses. For a given

Energy losses

For a given

species, energy losses become a limiting factor whenever E_{max}^{loss} , the energy such that $t_{acc}(E_{max}^{loss}) = t_{loss}(E_{max}^{loss})$, is lower than $E_{max}^{age} = Z \times R_{max}^{age}$ or $E_{max} = Z \times R_{max}^{conf}$. We will see that we expect this to be the case for electrons in SNRs, but not for protons or nuclei. Obviously for different type of astrophysical sources, the competition between the different causes of limitation of the maximum achievable energy has to be studied case by case for electrons, protons and nuclei⁶.

The formal definition for a given energy loss process i is :

$$t_{loss}^i(E) = \left(-\frac{1}{E} \left(\frac{dE}{dt}(E) \right)_i \right)^{-1} \quad (4.7)$$

when several energy loss processes have to be considered, we have :

$$t_{loss}^{total}(E) = \left(\sum_i \frac{1}{t_{loss}^i(E)} \right)^{-1} \quad (4.8)$$

Adiabatic losses

All charged particles in a supernova remnant (and in all expanding medium in general) are expected to experience adiabatic losses due to the expansion of the remnant. The gas does work during the expansion and its internal energy decreases : $dU = -PdV$ where U is the internal energy, P the gas pressure and V the volume. For a monoatomic gas $U = \frac{3}{2}nkJTV$ and $p = nkT$, with n being the particle density, T their temperature and k the Boltzmann constant, (the average energy per particle then being $\frac{3}{2}kT$). We then have, $dU = nVdE = -\frac{2}{3}nEdV$ and hence, $\frac{dE}{dt} = -\frac{2nE}{3N} \frac{dV}{dt}$, with $N = nV$.

$\frac{dV}{dt}$ is the expansion rate of the volume, which is related to the velocity field $\vec{v}(\vec{r})$. Let us now assume the volume is a cube, we can describe the change of the volume by the differential expansion of the three pairs of faces :

$$\frac{dV}{dt} = (v_{x+dx} - v_x)dydz + (v_{y+dy} - v_y)dx dz + (v_{z+dz} - v_z)dxdy \simeq \left(\frac{\partial v_x}{\partial x} + \frac{\partial v_y}{\partial y} + \frac{\partial v_z}{\partial z} \right) dxdydz = (\vec{\nabla} \cdot \vec{v})V \quad (4.9)$$

in the limit of small dx, dy, dz . We thus get, $\frac{dE}{dt} = -\frac{2}{3}(\vec{\nabla} \cdot \vec{v})E$.

For relativistic particles the energy per particle is $E = 3kT$, we thus get $\frac{dE}{dt} = -\frac{1}{3}(\vec{\nabla} \cdot \vec{v})E$.

Adiabatic losses

In the case of SNRs and more generally for astrophysical shock waves, we are dealing in good approximation, with uniformly expanding sphere, the velocity field is then $v(r) = v_0(r/R_{sphere})$, where R_{sphere} is the radius of the sphere and v_0 is the velocity at the outer radius R_{sphere} . In that case, we have $\vec{\nabla} \cdot \vec{v} = 3(v_0/R_{sphere})$ then for relativistic particles confined within the sphere we have :

$$-\left(\frac{dE}{dt}\right)_{exp} = \left(\frac{v_0}{R_{sphere}}\right) E = \left(\frac{1}{R_{sphere}} \frac{dR_{sphere}}{dt}\right) E \Leftrightarrow -\frac{1}{E} \left(\frac{dE}{dt}\right)_{exp} = \left(\frac{1}{R_{sphere}} \frac{dR_{sphere}}{dt}\right) \quad (4.10)$$

Adiabatic losses

The energy loss time is then $t_{loss}^{exp}(E) = \frac{\dot{R}_{sphere}}{R_{sphere}}$, which for a SNR within our notations corresponds to $t_{loss}^{exp}(E) = \frac{v_{sh}}{R_{sh}}$ which is equivalent to the age of the SNR in the free expansion phase. Adiabatic losses are then not a more limiting factor than the age of the SNR for the accelerated particles. Particles which are accelerated and manage to escape from the source will then not be very significantly affected by adiabatic losses. On the other hand, those which are accelerated but remain trapped within the SNR (because the rigidity they reached before being advected downstream of the shock is much lower than the R_{max}^{conf}) are likely to lose most of their energy while they are confined. Note that this energy is however not totally lost as far as cosmic-ray acceleration is concerned. It participates to the expansion of the SNR and might serve at later times to accelerate new cosmic-rays.

To conclude on adiabatic losses, let us note that the energy energy loss time is independent of the energy and that this process affects all types of relativistic charged particles the same way (protons, nuclei and electrons) and thus does not by itself break the symmetry in the behaviour of the different type of particles at a given rigidity.

Energy losses of electrons

Besides adiabatic losses, electrons are going to be affected by many different energy loss processes during their acceleration. To be more precise, these energy loss processes are not specific to electrons, they also affect protons and nuclei but in the case of SNR they are only significant for the case of electrons⁷. Among the most significant energy loss processes for electrons, one can cite :

- (i) Ionisation losses
- (ii) Bremsstrahlung losses
- (iii) Synchrotron losses
- (iv) Inverse compton losses

The first two processes are not too important in general in the case of SNR and we overlook them in the following. Note that all these processes are described in much more details in two very pedagogical books (in particular all the formulas we will give below are derived in all details), M. Longair's *"High Energy Astrophysics"* and Rybicki and Lightman's *"Radiative Processes in Astrophysics"*.

Synchrotron losses

In most cases, the most important energy loss process for electrons is the synchrotron emission which corresponds to the emission of an accelerated charged particle in the presence of an ambient magnetic field. It can be shown that :

$$-\left(\frac{dE}{dt}\right)_{syn} = \frac{4}{3}\sigma_T c \gamma^2 U_{mag} \quad (4.11)$$

where σ_T is the Thomson cross section, γ is the electron Lorentz factor and $U_{mag} = \frac{B^2}{2\mu_0}$ (S.I) = $\frac{B^2}{8\pi}$ (C.G.S) is the magnetic field energy density.

⁷In astrophysical sources where magnetic fields might be very strong, for instance in the nuclei of an AGN or a gamma-ray bursts, synchrotron losses become important for protons and nuclei (see below).

Synchrotron losses

For the energy loss time of the electrons by synchrotron losses, we get the following scaling law

$$t_{loss}^{syn}(E_e) = \left(-\frac{1}{E_e} \left(\frac{dE_e}{dt}(E_e) \right)_{syn} \right)^{-1} \simeq 1.2 \times 10^4 \left(\frac{B}{\mu\text{G}} \right)^{-2} \left(\frac{E_e}{10^{15} \text{ eV}} \right)^{-1} \text{ yr} \quad (4.12)$$

It can also be demonstrated that the typical energy of the synchrotron photons produced by an electron of energy E_e in a magnetic field B is given by :

$$E_{\gamma}^{syn}(E_e) \simeq 6.7 \times 10^4 \left(\frac{E_e}{10^{15} \text{ eV}} \right)^2 \left(\frac{B}{\mu\text{G}} \right) \text{ eV} \quad (4.13)$$

Let us add that the spectrum of photons produced by a population of electron is related to the spectrum of the parent population of electrons. Assuming the electrons are following a power law spectrum of index p : $n(E_e) \propto E_e^{-p}$, then the produced photon spectrum will also follow a power law : $n_{\gamma}(E_{\gamma}) \propto E_{\gamma}^{-\frac{p+1}{2}}$, *i.e* with a spectral index $\frac{p+1}{2}$.

Synchrotron losses

Let us come back to the case of a SNR with $B = 100 \mu\text{G}$ and $v_{sh} = 3000 \text{ km.s}^{-1}$ we see that $t_{loss}^{syn}(E_e = 10^{15} \text{ eV}) \simeq 1.2 \text{ yr} \ll t_{acc}(E_e = 10^{15} \text{ eV}) \simeq 480 \text{ yr}$. The energy for which $t_{loss}^{syn}(E_e) = t_{acc}(E_e)$ can be calculated, we see immediately that $E_{max}^{loss, syn} < 10^{14} \text{ eV}$ which means that the acceleration of electrons in a SNR will indeed be limited by synchrotron losses. If one assumes a stronger magnetic field, the situation only gets worse since $t_{loss}^{syn}(E_e) \propto B^{-2}$ while $t_{acc}(E_e) \propto B^{-1}$.

Let us now come back to the case of the SNR we considered earlier keeping the same physical parameters $B = 100 \mu\text{G}$, $v_{sh} = 3000 \text{ km s}^{-1}$, and the same time evolution using a free expansion phase duration of 480 years. Let us first calculate the value $E_{e max}^{loss, syn}$, the maximum energy of the electrons due to synchrotron losses, during the free expansion phase. Let us note that since the magnetic field is assumed to be constant during this phase then $E_{e max}^{loss, syn}$ should also be constant during the free expansion phase. Fixing $B = 100 \mu\text{G}$, we then have $t_{loss}^{syn} \simeq 1.2 \left(\frac{E}{10^{15} \text{ eV}} \right)^{-1}$ and $t_{acc} \sim 480 \text{ yr} \left(\frac{E}{10^{15} \text{ eV}} \right)$. Equating the two times gives us $E_{e max}^{loss, syn} \simeq 5 \cdot 10^{13} \text{ eV}$. This value of the maximum energy will hold till the end of the free expansion phase. To know the evolution of $E_{e max}^{loss, syn}$ during the Sedov-Taylor phase, we just have to calculate the scaling with time since we already know the value at the beginning of this phase :

Synchrotron losses

We have during the Sedov-Taylor phase, $t_{acc}(E_e) \propto E_e B^{-1} v_{sh}^{-2}$ and $t_{syn}(E_e) \propto E_e^{-1} B^{-2}$ which means, using the time evolution of B and v_{sh} , that $(E_{e\ max}^{loss, syn})^2 \propto B^{-1} v_{sh}^2 \Leftrightarrow E_{e\ max}^{loss, syn} \propto t^{-3/10}$. Summarising our results we have⁸ :

$$E_{e\ max}^{loss, syn}(t) \simeq 5 \cdot 10^{13} \text{ V for } t \leq 480 \text{ yr} \quad (4.14)$$

and

$$E_{e\ max}^{loss, syn}(t) \simeq 5 \cdot 10^{13} \times \left(\frac{t}{480 \text{ yr}} \right)^{-3/10} \text{ V for } t > 480 \text{ yr} \quad (4.15)$$

The evolution of $E_{e\ max}^{loss, syn}$ is shown in Fig. 4.3 and is compared to the evolution of E_{max}^{conf} and E_{max}^{age} allowing us to understand qualitatively the fate of the accelerated electrons during the whole SNR evolution.

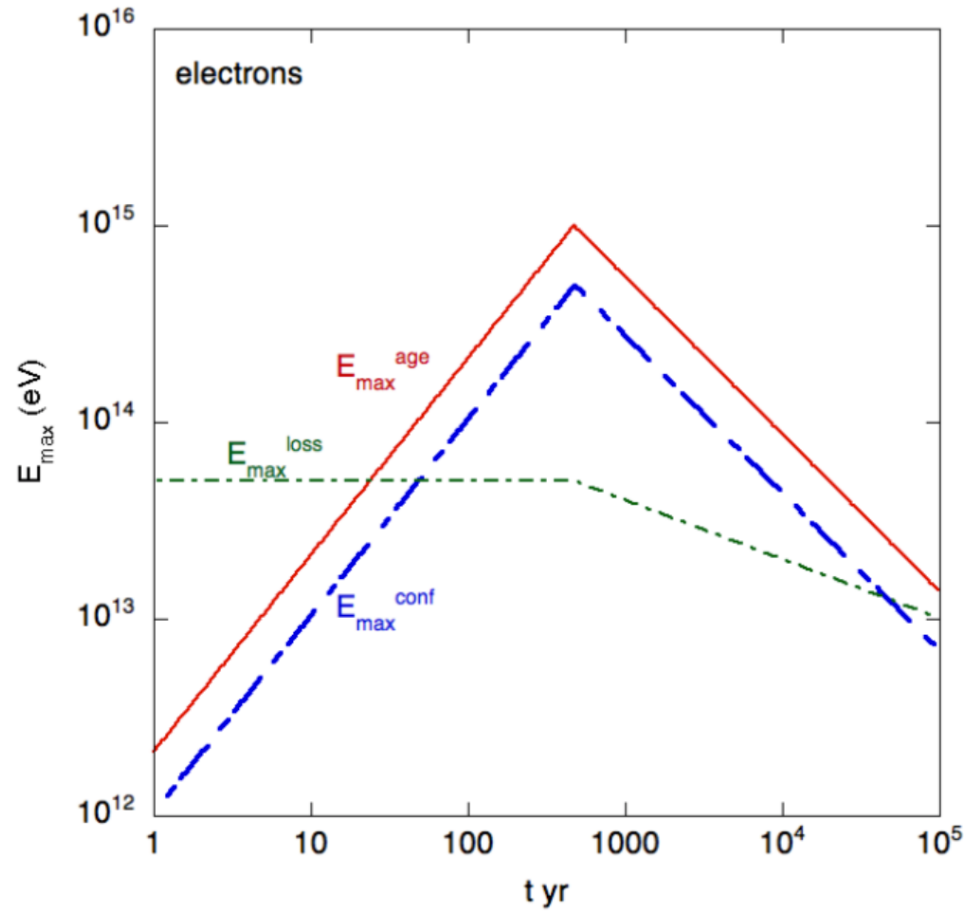


FIG. 4.3: Comparison of the time evolution of $E_{e \max}^{\text{loss, syn}}$, E_{\max}^{conf} and E_{\max}^{age} of the accelerated electrons for our toy model parameters (see text).

Synchrotron losses

During the beginning of the free expansion phase, $E_{e\ max}^{loss, syn}$ is larger than E_{max}^{conf} and E_{max}^{age} , as a result synchrotron losses are not a limiting factor for the acceleration of electrons and those with $E_e \simeq E_{max}^{conf}$ manage to escape to the ISM. This situation lasts roughly 50 years and then $E_{e\ max}^{loss, syn}$ becomes smaller than E_{max}^{conf} and E_{max}^{age} . In this case the acceleration of electrons is limited by synchrotron losses and moreover the electrons remain trapped in the SNR since $E_{e\ max}^{loss, syn}$ becomes rapidly significantly smaller than E_{max}^{conf} . This situation holds for the rest of the SNR evolution although with our hypothesis E_{max}^{conf} and E_{max}^{age} decrease more rapidly than $E_{e\ max}^{loss, syn}$ during the Sedov phase⁹.

This illustration demonstrate that synchrotron losses of electrons are a limiting factor for their acceleration during most of the evolution and incidentally these energy losses result in the production of ample fluxes of photons which as discussed earlier can be used to constrain the shape of the spectrum of the accelerated electrons (as well as some of the source parameters as we will see in the next few paragraphs).

Synchrotron losses

Finally it is worth mentioning that for a nuclear species of mass M and atomic number Z , the synchrotron loss time can be deduced from that of an electron of the same energy :

$$t_{syn}(E, M, Z) = \left(\frac{M}{m_e}\right)^4 \frac{1}{Z^4} t_{syn}(e^-, E_e = E) \quad (4.16)$$

Since $m_p/m_e \simeq 1836$ we immediately see that synchrotron losses will be negligible for protons and nuclei in SNRs.

Inverse Compton Losses

The energy lost per unit time by the inverse Compton process is given by :

$$-\frac{dE}{dt}(\gamma_e) = \frac{3}{4}\sigma_T c \gamma_e^2 U_{rad} \quad (4.18)$$

Where U_{rad} is the radiation energy density (for instance $U_{CMB} \simeq 0.25 \text{ eV cm}^{-3}$)

It yield for the energy loss time :

$$t_{loss}^{ICS}(\gamma_e) \simeq \frac{2.3 \times 10^{12}}{\gamma_e} \left(\frac{U_{rad}}{U_{CMB}} \right)^{-1} \text{ yr} \quad (4.19)$$

Let us note that in the ISM, synchrotron and inverse Compton losses are comparable while in a typical SNR synchrotron losses are far more important due to the amplified magnetic fields at play.

Inverse Compton Losses

There are basically two regimes for inverse Compton losses and photon emission depending on the above mentioned center of mass energy s .

(i) The Thomson regime is relevant when $s \simeq m_e^2 c^4$, we have in this case $\sigma_{ICS} \simeq \sigma_T$. In this case a photon with initial energy E_γ^{ini} is expected to be boosted to an energy $E_\gamma^{final} \simeq \gamma_e^2 E_\gamma^{ini}$ where γ_e is the Lorentz factor of the electron.

(ii) The Klein-Nishina regime is relevant when $s \gg m_e^2 c^4$. In this regime the cross section falls rapidly with s as $\sigma_{ICS} \propto s^{-1}$ and one gets $E_\gamma^{final} \simeq E_e$ meaning that the energy loss becomes catastrophic for the electron. Let us note that since we saw that the maximum energy of electrons in a SNR was quite unlikely to reach values larger than 10^{14} eV due to synchrotron losses then photons from ICS interactions in the Klein-Nishina regime are also very unlikely to reach these energies. This observation will actually be extremely relevant when we will discuss the possibility of distinguishing between high energy photons produced by high-energy electrons from those produced by high-energy cosmic-rays (see below).

Inverse Compton Losses

Like in the case of photons produced by synchrotron losses, the expected photon spectrum is related to the spectrum of the accelerated electron population which boosted them. Assuming again the accelerated electrons are following a power law spectrum of index p : $n(E_e) \propto E_e^{-p}$, then the produced photon spectrum will also follow a power law spectrum : in the Thomson regime, $n_\gamma(E_\gamma) \propto E_\gamma^{-\frac{p+1}{2}}$, and in the Klein-Nishina regime, $n_\gamma(E_\gamma) \propto E_\gamma^{-(p+1)}$.

Let us note that in some cases, the photons which are being boosted by the accelerated electrons might be the very same photons which have produced by the same population of electrons due to synchrotron losses. In this case, the ICS process is rather called synchrotron self-Compton or SSC¹⁰.

¹⁰Let us note that the ICS and synchrotron processes are always competing in astrophysical sources. If for instance the magnetic field is too strong and the high energy electrons lose their energy too rapidly by synchrotron losses then these "cooled" electrons are not available anymore to produce ICS photons in the Klein-Nishina regime and the latter process is then highly suppressed.

In the case of protons and nuclei the ICS process is totally negligible.

Energy losses of protons and nuclei

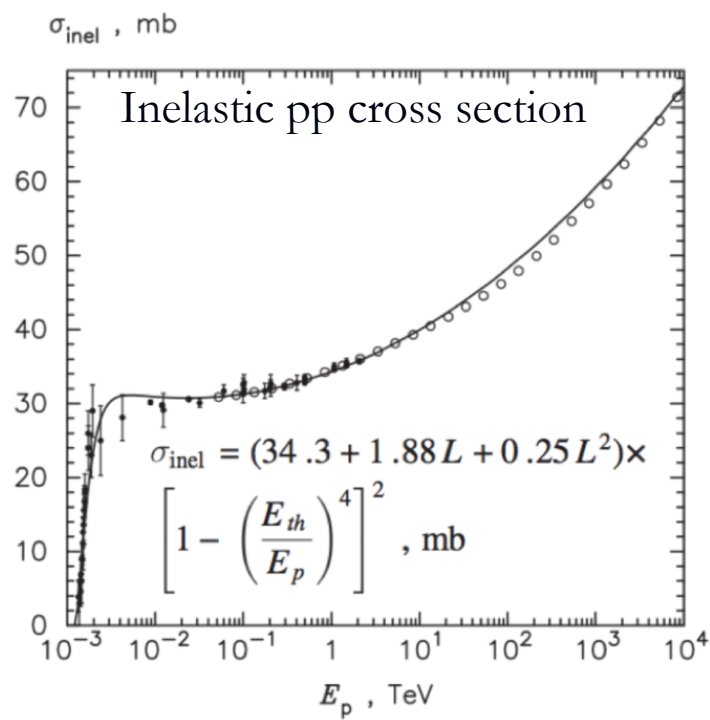
As discussed above, protons and nuclei suffer from adiabatic losses but remain quite insensitive to synchrotron (at least in SNRs) and ICS losses. The main interaction channel for protons and nuclei takes place through hadronic interactions¹¹ with the ambient matter (mainly H and He atomic nuclei) which is in good approximation at rest. In the case of protons, above a certain energy threshold pions can be produced (see below) while nuclei suffer from spallation reactions (see Chapt. 2) and may also emit pions.

Let us concentrate on the proton case (so-called pp interactions). A collision between an accelerated proton and an ambient proton or He at rest gives in most cases a pion (either charged or neutral) :

$$p + p \rightarrow p + p + \pi^0 \Rightarrow \pi^0 \rightarrow 2\gamma \quad (4.20)$$

$$p + p \rightarrow p + p + \pi^+ \Rightarrow \pi^+ \rightarrow \mu^+ + \nu_\mu \Rightarrow \mu^+ \rightarrow e^+ + \bar{\nu}_\mu + \nu_e \quad (4.21)$$

$$p + p \rightarrow p + p + \pi^- \Rightarrow \pi^- \rightarrow \mu^- + \bar{\nu}_\mu \Rightarrow \mu^- \rightarrow e^- + \nu_\mu + \bar{\nu}_e \quad (4.22)$$



Energy losses of protons and nuclei

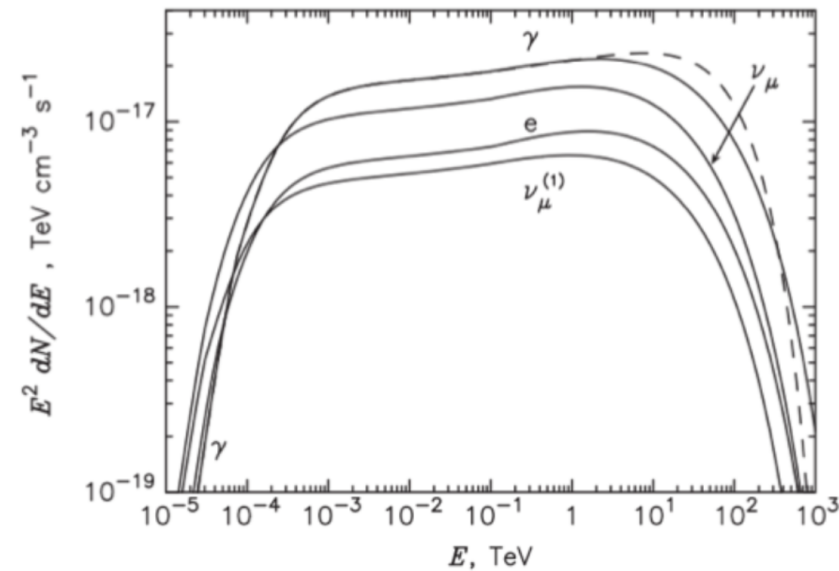
The energy threshold to produce a π^0 in pp interactions is :

$$E_p^{th} = m_p + \frac{m_{\pi^0}}{m_p} \left(2m_p + \frac{m_{\pi^0}}{2} \right) \simeq 1.22 \text{ GeV} \quad (4.23)$$

which correspond to a kinetic energy of the proton $T_p^{th} \simeq 280 \text{ MeV} \simeq 2m_{\pi^0}$.

In good approximation, the produced π^0 carries in average $\sim 17\%$ of the accelerated proton initial energy which redistributed to the 2 photons immediately produced in the π^0 decay. The pp cross section shown in Fig. 4.4a is quasi constant with the energy (hardly rising by a factor of two over 7 orders of magnitude of the proton energy), for the following orders of magnitude calculations we will assume the cross section to be constant at 50 mbarn.

Energy losses of protons and nuclei



Spectrum of photons, electrons, neutrinos (electronic and muonic) produced by the interaction of protons distributed as a power law spectrum $n(E) \sim E^{-2}$ with an exponential cut-off above 10^{14} eV (100 TeV).

The spectrum of outgoing photons, neutrinos and electrons after pp interactions are shown in Fig. 4.4b, assuming an initial spectrum of accelerated protons $n(E_p) \propto E^{-2}$ and an exponential cut-off above 10^{14} eV (100 TeV). The resulting photon spectrum has practically a shape in $n(E_\gamma) \propto E_\gamma^{-2}$, although slightly harder (*i.e.* $p \leq 2$) due to slight increase of the pp cross section with E_p . We also see that the photon spectrum shows an exponential cut-off around ~ 10 TeV (10^{13} eV) which is expected since photons carry roughly a bit less than 10% of the initial accelerated proton energy (and the proton spectrum was assumed to present an exponential cut-off above 100 TeV). Note that the situation of the produced neutrinos is qualitatively the same except that these neutrinos are expected to carry 3-5% of the energy of the primary proton.

Energy losses of protons and nuclei

With the cross section being known, one can calculate the mean interaction time $t_{int}^{pp} = (n\sigma_{pp}c)^{-1}$. Using $\sigma_{pp} \simeq 50$ mbarn (and constant), we get

$$t_{int}^{pp} \simeq 2.1 \times 10^6 \left(\frac{n}{10 \text{ cm}^{-3}} \right)^{-1} \text{ yr} \quad (4.24)$$

since in average 17% of the proton energy is lost during a single interaction we get for the loss time t_{loss}^{pp} ,

$$t_{loss}^{pp} \simeq 10^7 \left(\frac{n}{10 \text{ cm}^{-3}} \right)^{-1} \text{ yr} \quad (4.25)$$

The loss time is much larger than the time a SNR remain active. It means that hadronic interactions are never a limiting factor for the acceleration of protons (it remains true for nuclei, the cross section being roughly proportional to $A^{2/3}$). However, the photons which are emitted during the interactions (which are unlikely during the acceleration of a single proton or nuclei but must occur within a large population of accelerated protons and nuclei) can be used as a signature of the presence of accelerated cosmic-ray protons and nuclei.

Leptonic/hadronic γ emission

The produced photons will however have to compete with those emitted by electrons in the same energy range. Even though electrons are in principle discriminated at the injection at the shock (see the paragraph on "non-trivial issues") with respect to protons and nuclei, they radiate so much more efficiently that it is always quite challenging to find protons and nuclei acceleration signatures in the photon spectra emitted by SNRs. We will see a few examples in the next paragraphs.

Leptonic/hadronic γ emission: RX J0852.0-4622 (Vela-Jr) SNR

The complexity of the interpretation of photon spectra observed from SNRs can be illustrated by the case of the SNR RX J0852.0-4622 also called Vela-Jr shown in Fig. 4.5. This SNR has been observed in radio, X-rays and very high energy γ -rays (by the HESS observatory)¹². The SNR distance and the physical environment (matter density, magnetic fields) are not very well constrained by observations. In the case, there is a large room to model the γ -ray emission and Fig. 4.5 shows two different models which can be considered as acceptable fits of the data. The left panel assumes a predominantly "leptonic" origin (*i.e* a majority of photons emitted by accelerated electrons) of the γ -ray assuming a relative small value of the field $B = 6 \mu\text{G}$ (so more or less comparable with that of the ISM) in the acceleration region, together with a low matter density $8 \cdot 10^{-3} \text{ cm}^{-3}$ to favor inverse Compton emission over π^0 decay. On the other hand, the right panel with much larger magnetic field $B = 85 \mu\text{G}$ and density $d = 2 \text{ cm}^{-3}$ (closer to the standard value expected especially in the context of amplified magnetic fields at the shock) implies a dominant contribution of "hadronic" γ -rays (*i.e* produced by hadronic interactions) from the decay of π^0 .

Leptonic/hadronic γ emission: RX J0852.0-4622 (Vela-Jr) SNR

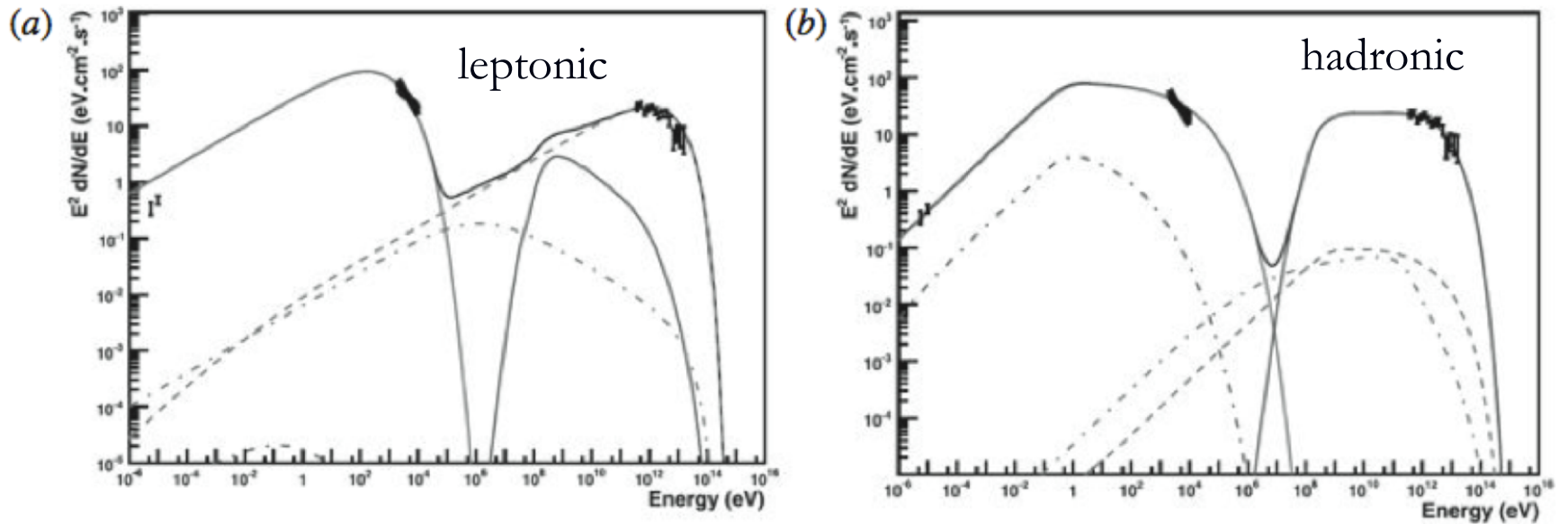


FIG. 4.5: Photon spectrum observed in radio, X-rays and γ -ray (HESS) from the RX J0852.0-4622 (Vela-Jr) SNR. Data points are compared with predictions assuming a leptonic (left) and a hadronic (right) origin of the γ -ray emission (see text).

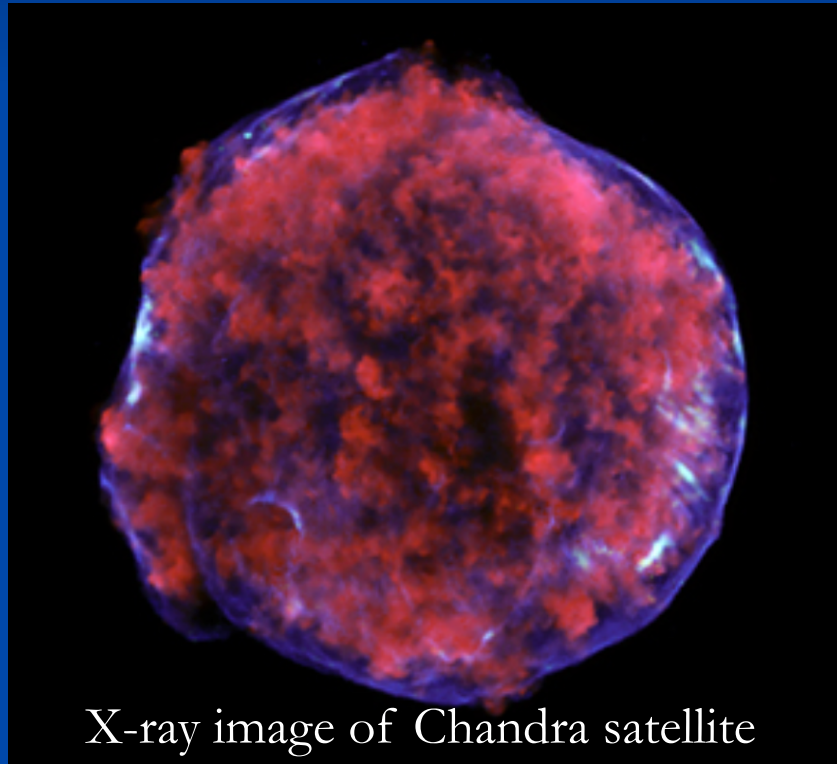
Leptonic/hadronic γ emission: RX J0852.0-4622 (Vela-Jr) SNR

The paucity of the informations on the SNR environment (as in 2007) as well as the very partial measurements of the multiwavelength photon spectrum makes the origin of the γ -ray signal difficult to determine with certainty. Let us note that, even assuming a hadronic origin of the γ -ray photons the fact that no photons were detected above ~ 20 TeV ($2 \cdot 10^{13}$ eV) implies that there is in any case no signature of the acceleration of cosmic-rays above a few 10^{14} eV, which represents an energy scale \sim an order of magnitude below the knee energy.

We started our brief tour of SNR observations by a relatively ambiguous case. For some SNRs the distinction between the leptonic or hadronic origin of the high energy photon signal can however be much clearer.

The Tycho SNR

The Tycho SNR is very well known, it corresponds to the remnant of the Tycho supernova which could be observed with the naked eyes in the years 1572.



X-ray image of Chandra satellite

The Tycho SNR

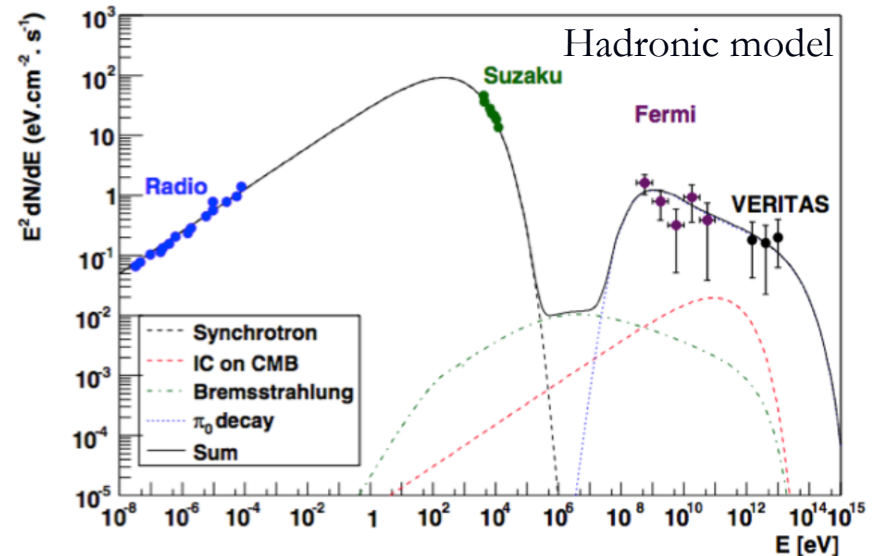
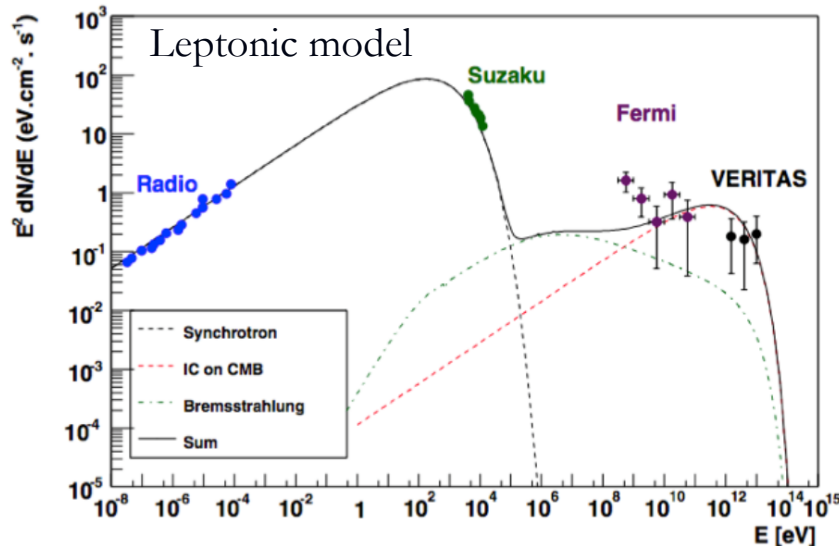
The emission spectrum is

now well measured in radio and X-rays (these emissions are interpreted as the synchrotron emission of accelerated electrons) allowing to constrain the value of the ambient magnetic which is found to be of the order of $B \sim 215 \mu\text{G}$ (which correspond to a strong amplification with respect to the ISM magnetic field). With such an important constraint, the determination of the origin of the γ -ray signal measured by both Fermi (below 100 GeV) and VERITAS (above 100 GeV) is easier although the distance of the remnant is not precisely known. As shown in Fig. 4.6, the best fit of

The Tycho SNR

The best fit of the multiwavelength data are obtained with models assuming a dominant contribution of hadronic processes. the spectral index found for the accelerated protons is $p' \approx 2.3$ which is, as it should be (at least assuming acceleration by DSA), the same as the one of the electrons constrained by radio and X-ray data.

Leptonic models on the other hand give a much worse agreement with the data even though the model displayed allowed for a significant decrease of the assumed magnetic field (with respect to the favored value of $B \approx 215 \mu\text{G}$)



Tycho SNR thus represent a case where we have very strong evidence of the acceleration of cosmic- rays in a SNR. Let us note however that no photon signal is observed above a few 10 TeV which means again that there is no signature of the acceleration of cosmic-rays above a few 10^{14} eV in this SNR

The RX J1713.7-3946 SNR

In the case of the SNR RX J1713.7-3946, a different conclusion is reached. This well known SNR is older than Tycho's SNR (~ 1700 years old) which means that this SNR is well within its Sedov phase (unlike Tycho's SNR which has entered the Sedov-Taylor phase). For RX J1713.7-3946, X-ray measurement point to a magnetic field of the order of $10 \mu\text{G}$ only slightly large than in the ISM. The γ -ray spectrum has been measured between $\sim 1 \text{ GeV}$ and 100 TeV by Fermi and HESS.

In this case, as can be seen in Fig. 4.7, it seems that leptonic models for which the γ -ray emission is dominated by the ICS emission of the accelerated electrons give a much better fit of the data. With such a low value of the magnetic field, it is indeed easier for the ICS emission to overwhelm the contribution from π^0 . The dominant contribution of the leptonic signal of course does not mean that cosmic-ray nuclei are not accelerated in this SNR, but there is no course no clear signature of this acceleration in the observed photon spectrum.

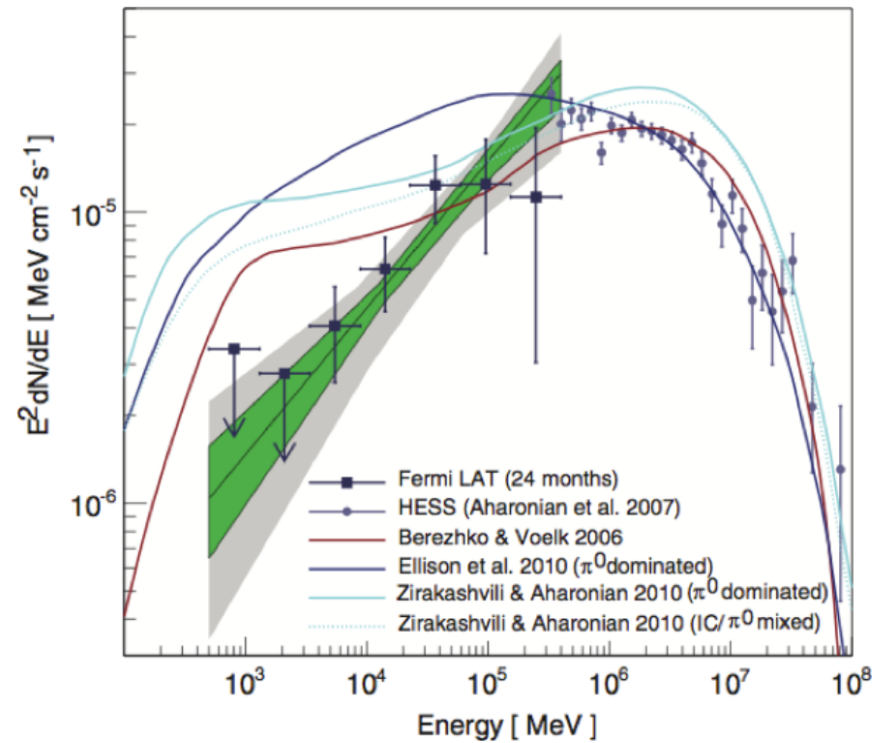
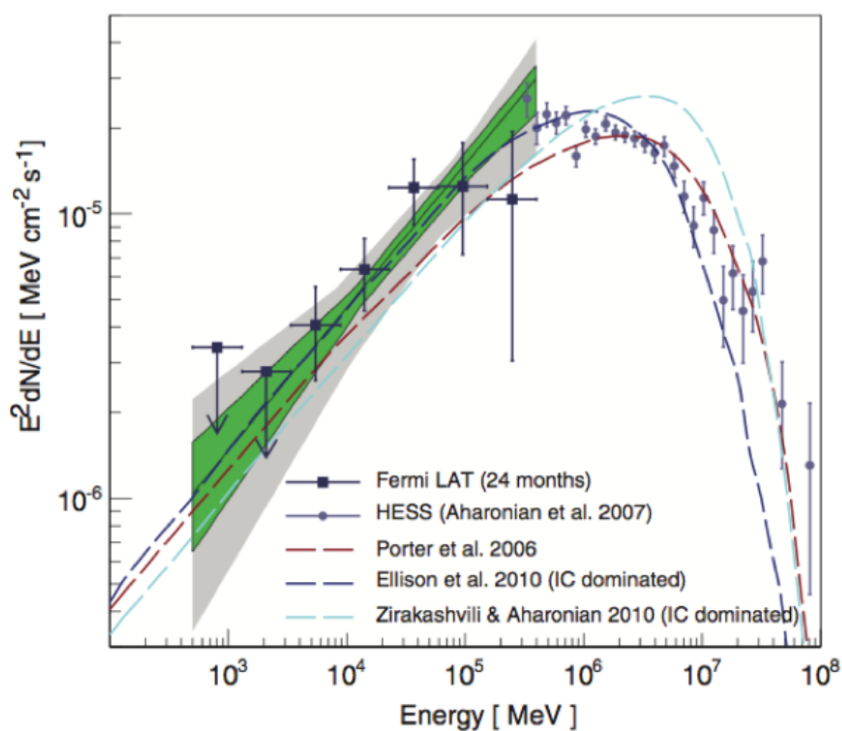
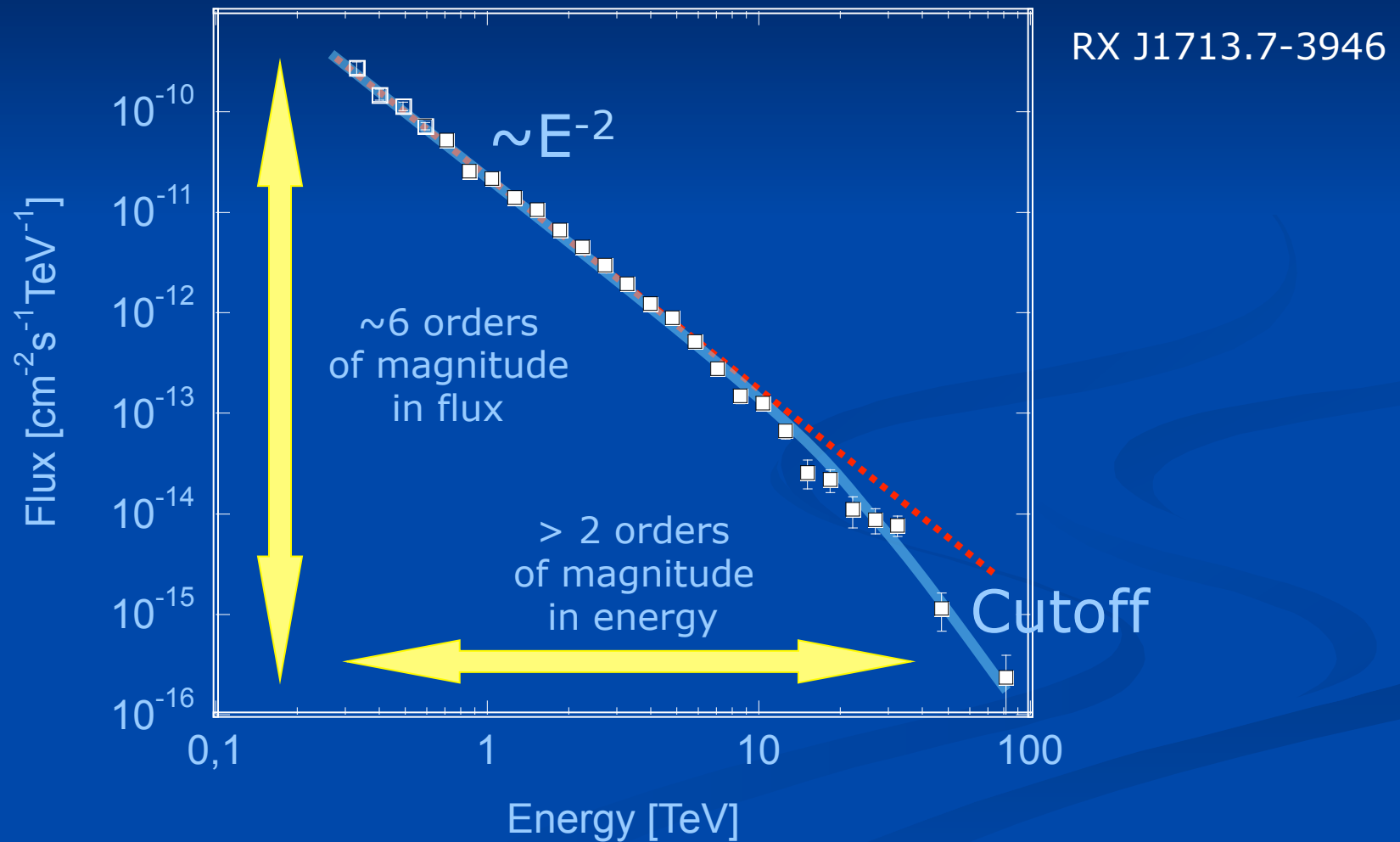


FIG. 4.7: Photon spectrum observed in γ -rays (Fermi and HESS) from the RX J1713.7-3946 SNR. Data points are compared with predictions assuming a leptonic (left) and a hadronic (right) origin of the γ -ray emission (see text).

Spettro energetico RX J1713.7-3946



SNRs and galactic cosmic rays

During the last few years and the emergence of high aperture and high resolution γ -ray observatories, the number of SNRs observed in γ -rays as well as the quality of the observations, increased significantly. A few tens of SNRs have now a well measured γ -ray photon spectrum. Among them some favour a leptonic origin of the signal while other favour a hadronic origin.

Although it is now clear that SNRs do accelerate some cosmic-rays ¹⁴, in the current situation it is extremely difficult to conclude on whether or not SNRs are the main sources of Galactic cosmic-rays. In particular, with current observations there is no photon signature of the fact that SNR are able to accelerate cosmic-rays beyond a few 10^{14} eV. Furthermore, the maximum energies of some SNRs (like Tycho and CasA) at the transition between the free expansion and the Sedov-Taylor phase as constrained by their X-ray rims seem indeed to be significantly lower than the knee energy. As we will see in the next few paragraphs this is in principle a problem since a good candidate for the title of "main source of the Galactic cosmic-rays" should be able to accelerate cosmic-rays at least up to the knee energy.

SNRs and galactic cosmic rays

Now one must be extremely careful in interpreting the γ -ray spectra, we just discussed since in principle they are representative of the accelerated particles population at a given time of the SNR evolution. These spectra are just telling us that at the (retarded) time of the observations, there is no sign of protons being accelerated above a few 10^{14} eV. It is not telling us anything about the population of cosmic-rays which are escaping to the ISM (since those that emit γ -ray are still inside the SNR), nor is it telling us anything about what the accelerated cosmic-ray population was at earlier times of the SNR evolution.

Taking at face value the toy model of a SNR evolution we discussed in the previous paragraphs, Tycho SNR or other well known and well observed SNRs like CasA, which are both more or less at the transition between the free expansion and the Sedov-Taylor, should be at the stage of their evolution at which the maximum energy of the accelerated cosmic-rays reaches its highest value. In the framework of this particular model of the SNR evolution the non observation of photon signature of the acceleration of cosmic-rays above 10^{14} eV would indeed indicate that they should never be able to reach much higher energies during their whole evolution.

SNRs and galactic cosmic rays

It is important to note that very different models for the evolution of the SNR, especially with respect to the maximum energy reachable by cosmic-rays have emerged in the past few years. Some of these models in particular predict that the production of very high energy cosmic-rays (well above 10^{15} eV) is possible during the very early times of the shock propagation (the very first few years or even on shorter time scales). These models invoke initially extremely strong magnetic fields (a few tens of Gauss !) decaying like t^{-1} (for which there exist some observational evidences in some rare type, exceptionally bright extragalactic supernovae). For this class of models it is normal not to observe any signature of cosmic-ray acceleration above 10^{15} eV since these signatures could only be found during a short period of time after the supernova event. The Galactic SNRs we observe in γ -rays all being much too old to present these signatures. Observation of larger samples of SNRs (especially younger SNRs) by the next generation of γ -ray observatory will certainly be required to further test the relevance of these more recent models. Molecular clouds we will discuss in the next paragraph also represent potentially powerful probes of both the cosmic-ray escape and the maximum acceleration energy.

SNRs and galactic cosmic rays

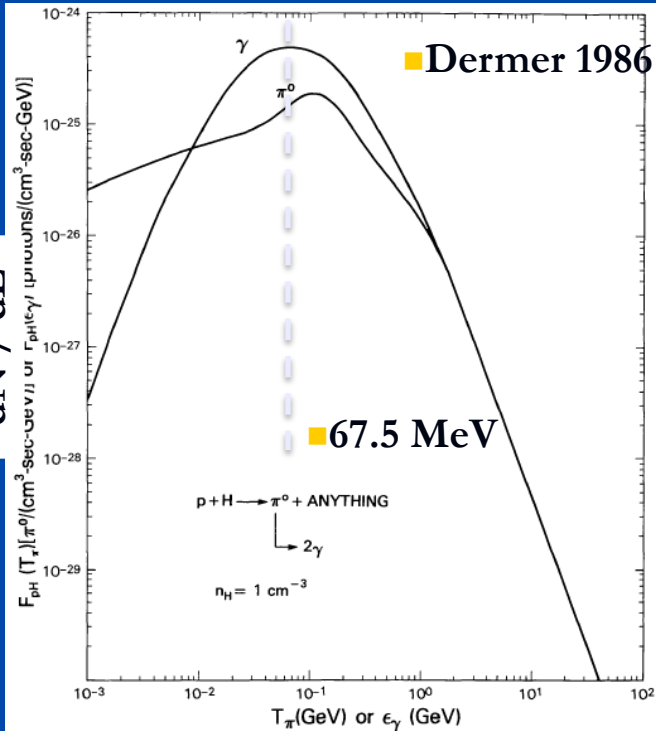
We must conclude that the nature of the main source of Galactic cosmic-rays is currently unclear. Although SNR still remain the most popular candidate, some authors have argued that scenarios involving super bubbles could solve most of the caveats encountered with the SNR scenario 15 but observational signatures are still needed to lend further weight to this possibility.

Molecular clouds as diagnostic tool for the spectrum of escaping CR

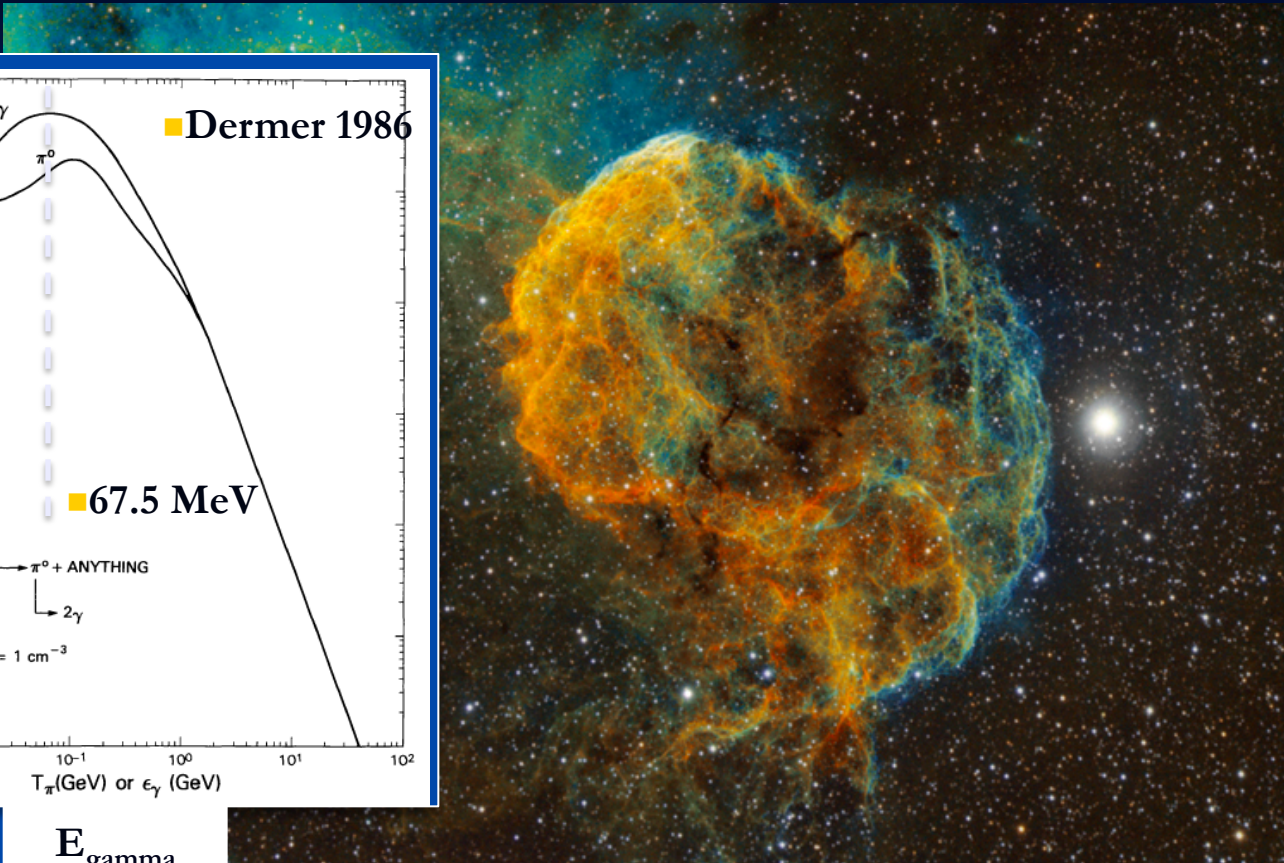
As discussed above multi-wavelength spectra give precious informations on the population of accelerated particles present in a SNR at a given time. Moreover, the observation of SNR of different ages gives us some hint of how these populations are evolving with time. However, these observations do not give any direct indication of the spectrum of cosmic-rays which are escaping from the SNR environment. This fact is of course problematic since these escaping cosmic-rays are precisely those which might eventually arrive on Earth after propagation in the ISM. As seen in Chapt. 1, the diffuse γ -ray emission associated with the Galactic plane is due to hadronic interactions of cosmic-rays with the ISM. Although this emission brings us informations on the propagation of these cosmic-rays in the Galaxy, this diffuse emission does not allow to put strong constraints on cosmic-ray origin.

Of course stronger γ -ray emission is expected denser regions of the ISM like molecular clouds (see Chapt. 1) which can locally reach densities of the order of 10^6 cm^{-3} . It is interesting to note that molecular cloud are often located in (or in the vicinity of) star forming regions meaning that there is a non negligible probability for molecular clouds to be found in the vicinity of SNRs. In this case, the flux of cosmic-rays entering the molecular cloud would be dominated by the contribution of the nearby SNR. The pp interactions in the molecular cloud and the consecutive γ -ray emission could be interpreted as the signature of escaping cosmic-rays from the nearby SNR environment and give precious informations about their energy.

dN / dE



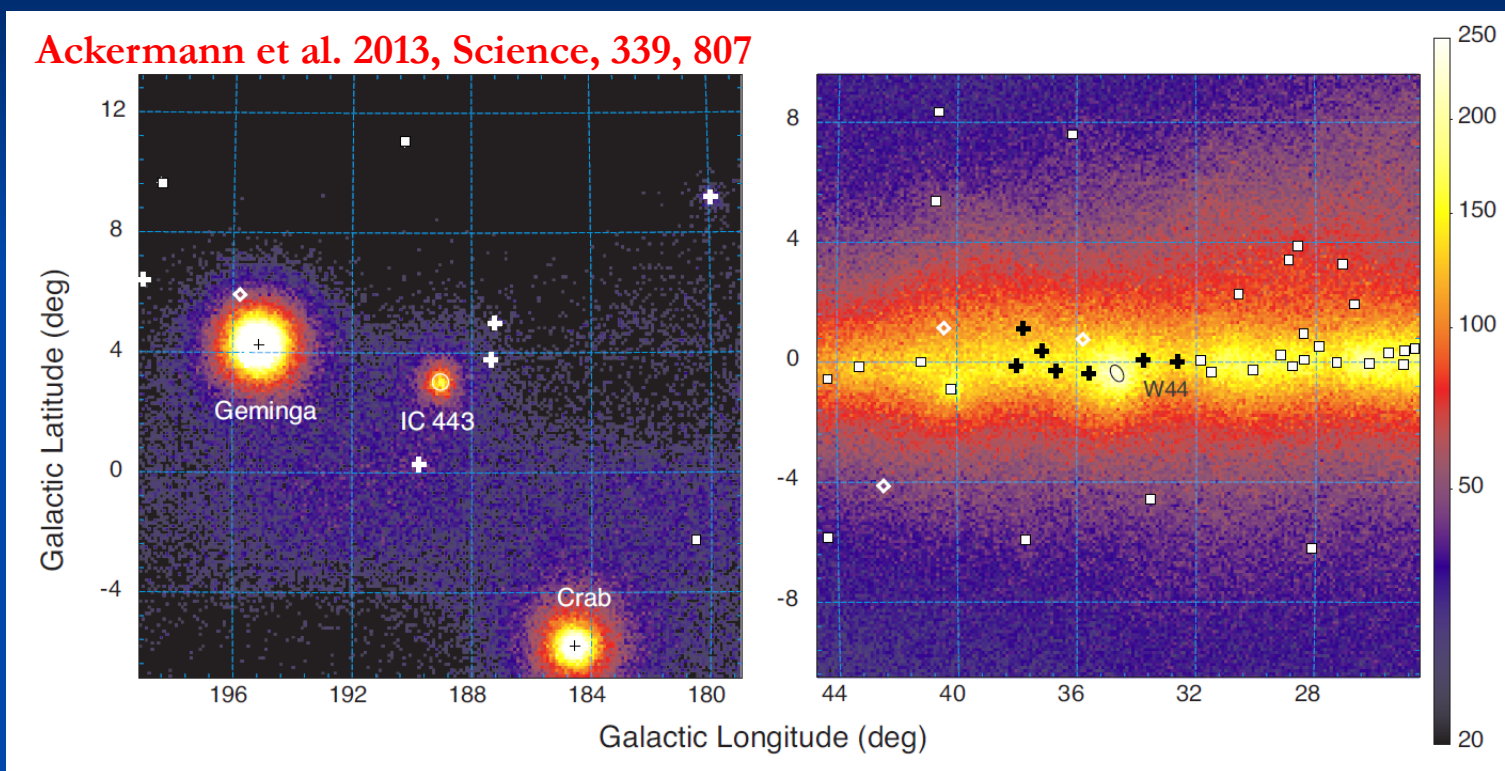
E_{gamma}



DETECTION OF THE PION- DECAY CUTOFF IN SUPERNOVA REMNANTS

Top SNR Candidates: IC 443 & W44

Both SNRs interacting with clouds, ages of $\sim 10^4$ years,

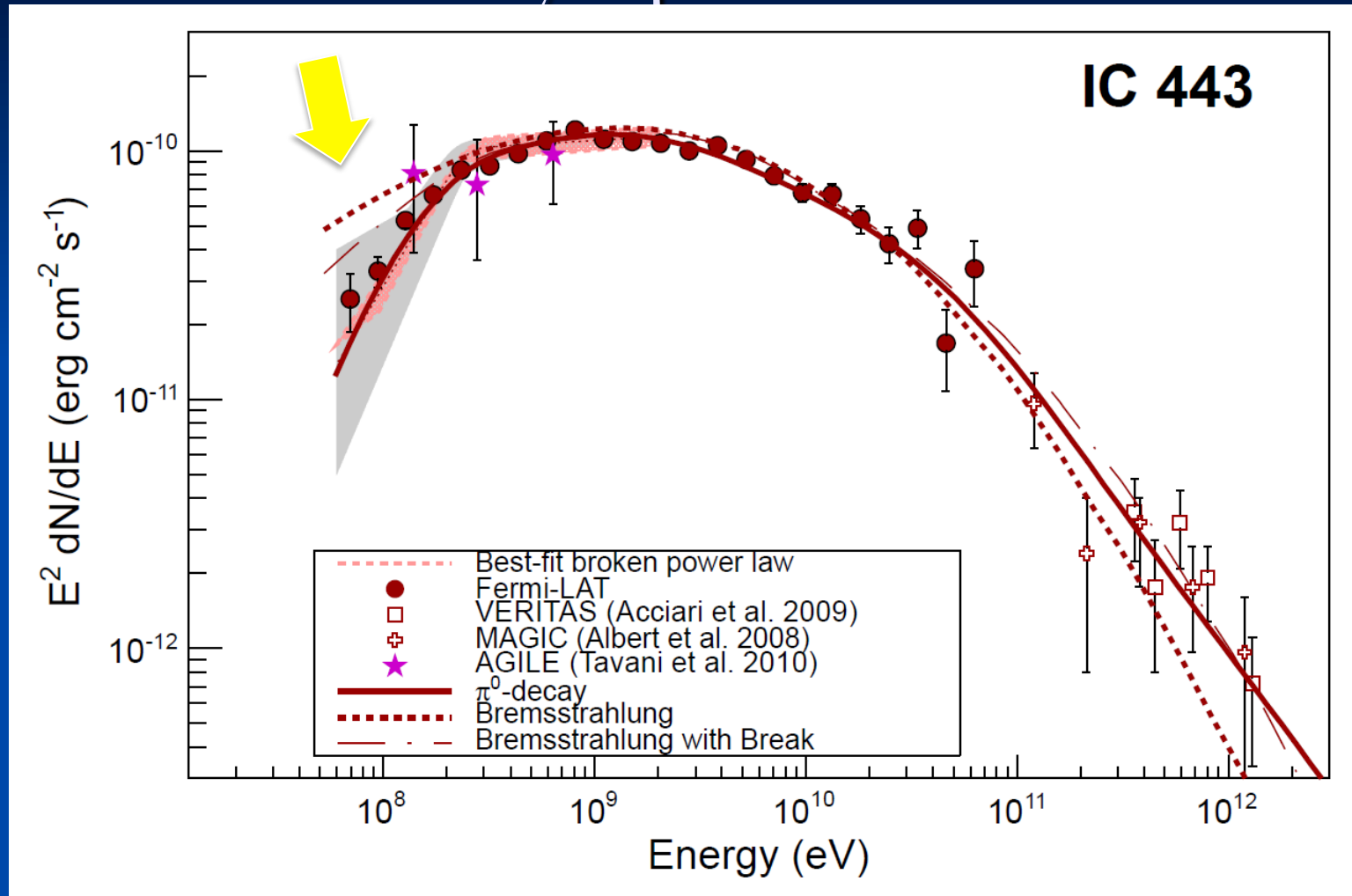


■ Counts map in 0.1 deg x 0.1 deg pixels, 60 MeV – 2 GeV

■ Diamonds indicate previously undetected sources

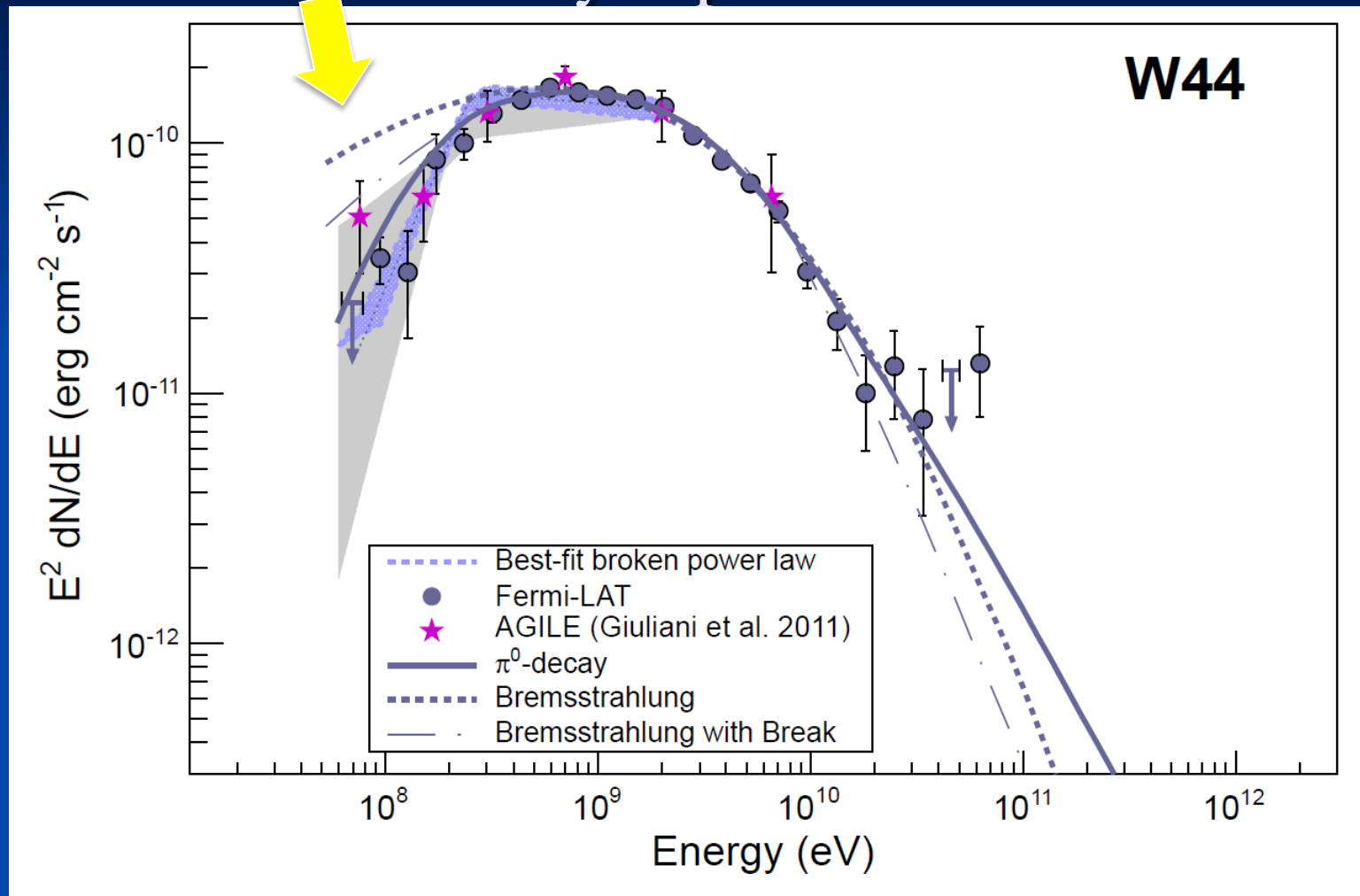
■ Crosses and diamonds indicate sources with normalization free in the fit

Gamma-ray Spectrum IC 443



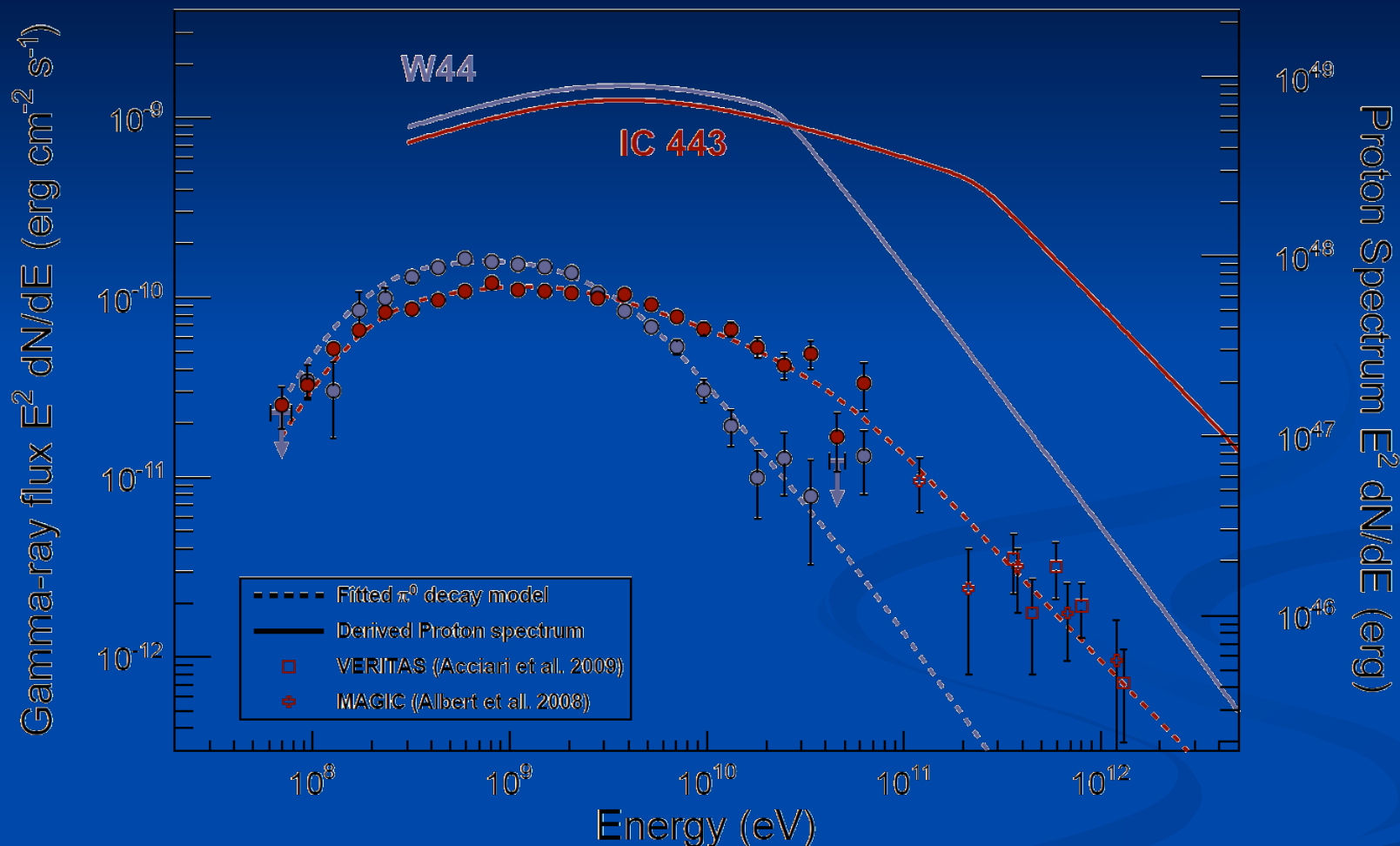
- Color (Gray) shaded region indicates statistical (systematic) uncertainty < 2 GeV.
- Systematic uncertainty associated with Galactic diffuse modeling was estimated by using several alternative diffuse models based on GALPROP.
- Ackermann et al. 2013, Science, 339, 807

Gamma-ray Spectrum W44



- Color (Gray) shaded region indicates statistical (systematic) uncertainty < 2 GeV.
- Systematic uncertainty associated with Galactic diffuse modeling was estimated by using several alternative diffuse models based on GALPROP.
- Ackermann et al. 2013, Science, 339, 807

Gamma-ray and Inferred Proton Spectra



Assume average gas densities of 20 cm^{-3} (IC 443) and $n = 100 \text{ cm}^{-3}$ (W44) and distances of 1.5 kpc (IC 443) and 2.9 kpc (W44), factor 1.85 enhancement from heavier nuclei. Inferred CR acceleration efficiencies of 1-10% (protons with $p > 0.8 \text{ GeV c}^{-1}$).

The knee of the CR spectrum

Before closing our discussion of SNRs, it is useful to discuss the origin of the knee of the cosmic-ray spectrum to better understand some aspects we discussed in the previous paragraphs. We first remind that in the context of the leaky box model assuming a steady state we obtained in Chapt. 2, for a given nuclear species i :

$$0 = q_i(R) - \frac{N_i(R)}{\tau_{esc}(R)} \Leftrightarrow N_i(R) = q_i(R)\tau_{esc}(R) \quad (4.26)$$

The knee is a feature of the cosmic-ray spectrum (a steepening) observed on earth (see Fig. 4.13), one sees in Eq. 4.26 that this feature can come either from a change in the source term or in the escape term.

The knee of the CR spectrum

(i) In the case, the source term is involved, one could guess that the main sources of Galactic cosmic-rays are reaching their maximum energy at the knee, causing a feature in the spectrum. In this case, since the different species are expected to be accelerated to the same maximum rigidity (since we showed that energy losses were likely not to be a limiting factor for Galactic cosmic-ray acceleration), then the knee would more precisely mark the maximum energy of the proton component (which is the most abundant species), followed by the other species at energies $E_{max}(Z) = Z \times E_{max}(proton) = Z \times E_{knee}$. This behaviour is schematized in Fig. 4.13, where fictitious spectra of the most abundant species are depicted for illustrative purpose. Let us note that in this case, even if the proton component has a sharp cut-off above its maximum energy, the total spectrum will remain relatively smooth since the different species will experience their own knee at energies which are proportional to their charge.

Now of course, for this scenario to hold one needs the main sources of Galactic cosmic-rays to be able to accelerate protons at least up to the knee energy, which seems to be a bit challenging for SNR at least for models predicting that the highest value of the maximum energy is reached at the transition between the free expansion and the Sedov-Taylor phases.

(ii) On the other hand, it is also possible that the knee could be due to a change in the energy evolution of the escape term. In Chapt. 2, we saw that $\tau_{esc}(R) \propto D(R)^{-1}$ where D is the diffusion coefficient. We also saw that the rigidity evolution of the diffusion coefficient was expected to show an inflexion^{*} around the rigidity at which $r_L(R) \simeq \lambda_c$ (λ_c , being the coherence length of the field) as can be seen in Fig. 2.9. In the Galaxy we have roughly $B \simeq 3 - 10 \mu\text{G}$ and $\lambda_c \simeq 1 - 10\text{pc}$. Taking the values $3 \mu\text{G}$ and $\lambda_c = 1 \text{ pc}$ we see that the rigidity for which $r_L(R) \simeq \lambda_c$ is $\sim 3 \cdot 10^{15} \text{ V}$ which is close to the knee energy (for protons). Assuming the knee is indeed due a change in the rigidity evolution of the diffusion coefficient, since the rigidity is the relevant parameter, we would also expect first a change in the proton component and then changes in the behaviour of the other species at energies proportional to their charge (the schematic view in Fig. 4.13 would still hold qualitatively¹⁶).

Assuming the knee is purely due to the evolution of $\tau_{esc}(R)$ (and then of $D(R)$) then the source term would have to remain unchanged at the knee meaning that in this case the maximum energy of the main sources of Galactic cosmic-rays would have to be higher than the knee and probably even significantly higher. This eventuality is of course even more problematic for SNRs.

^{*}The diffusion coeff may vary if the magnetic field power spectrum changes

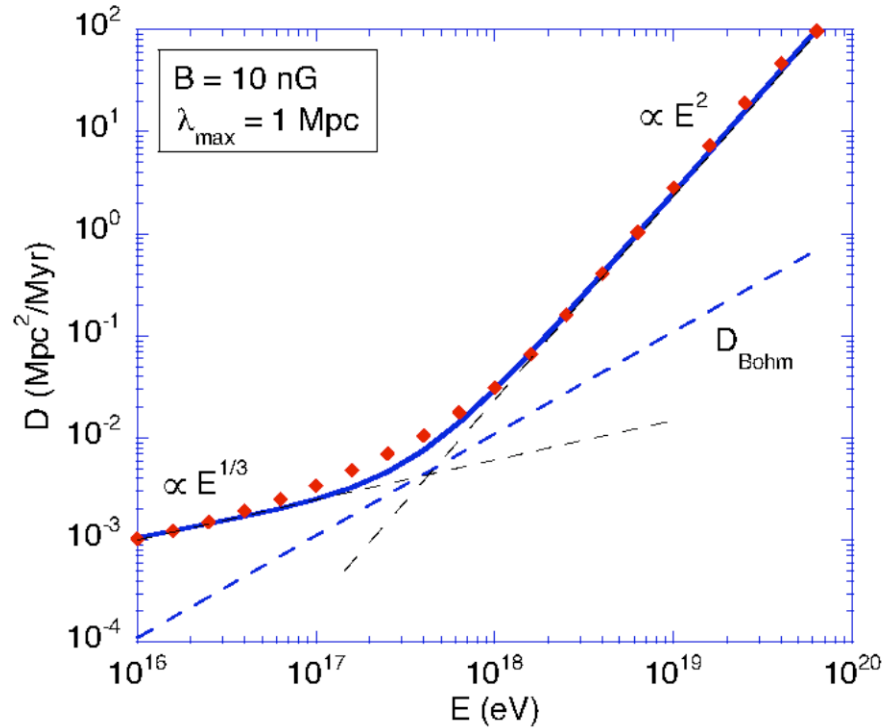


FIG. 2.9: Diffusion coefficient of protons as a function of energy, for a turbulent magnetic field $B = 10 \text{ nG}$ and $\lambda_{\text{max}} = 1 \text{ Mpc}$. The red dots are the computation results, with asymptotic behaviors indicated by the thin dashed lines. The Bohm diffusion coefficient is also shown for comparison (dashed line), the latter can be disregarded until we come to Chapter 3.

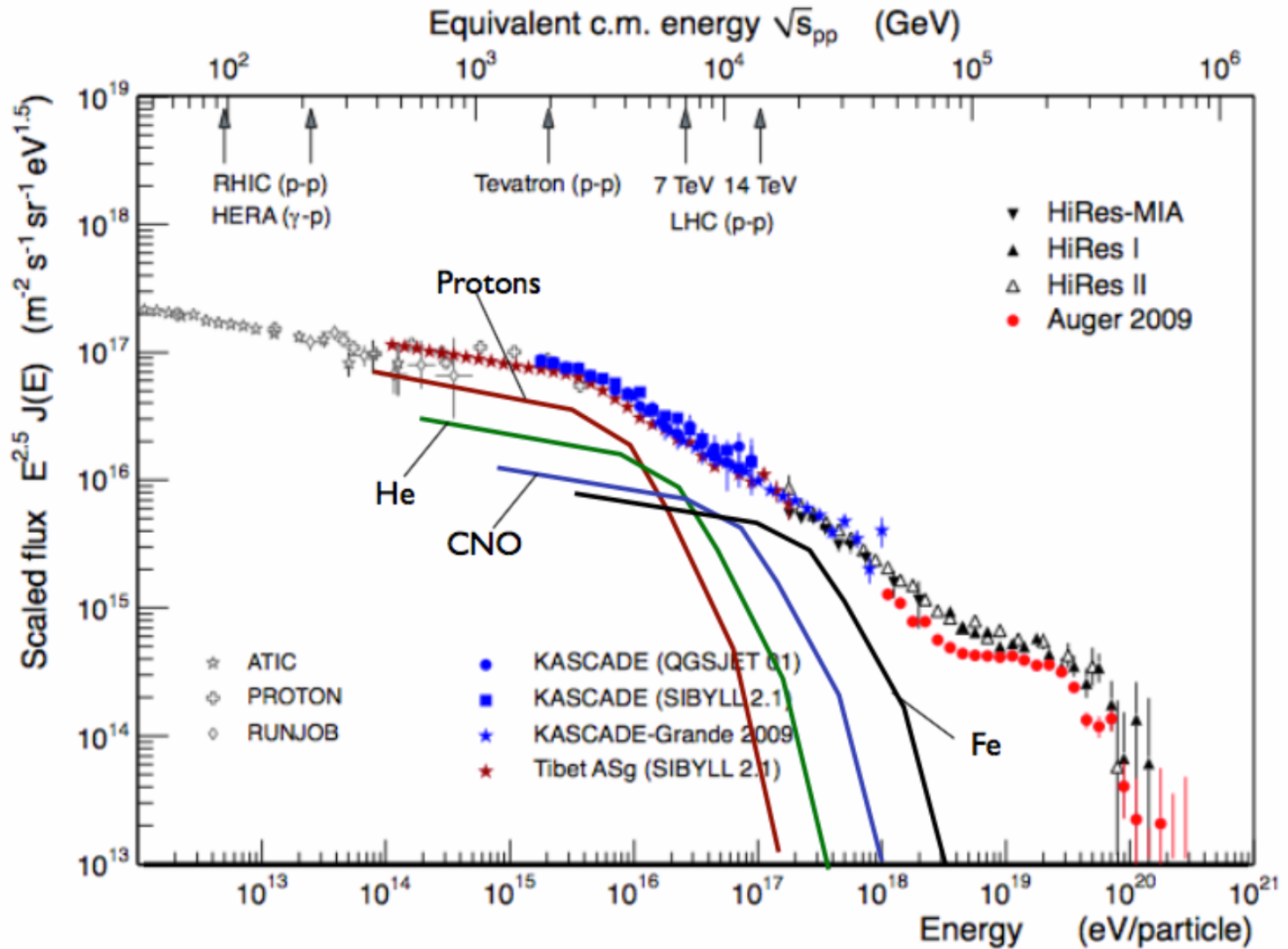


FIG. 4.13: Same as Fig. 2.2. In addition fictitious spectra of the most abundant species have been added to illustrate the idea of the successive knees of the different species at energies $E_{knee}(Z) = Z \times E_{knee}(\text{proton}) = Z \times E_{knee}$.